

Community detection in multi-layer networks by regularized debiased spectral clustering

Huan Qing^{a,*}

^a*School of Economics and Finance, Lab of Financial Risk Intelligent Early Warning and Modern Governance, Chongqing University of Technology, Chongqing, 400054, China*

Abstract

Community detection is a crucial problem in the analysis of multi-layer networks. In this work, we introduce a new method, called regularized debiased sum of squared adjacency matrices (RDSoS), to detect latent communities in multi-layer networks. RDSoS is developed based on a novel regularized Laplacian matrix that regularizes the debiased sum of squared adjacency matrices. In contrast, the classical regularized Laplacian matrix typically regularizes the adjacency matrix of a single-layer network. Therefore, at a high level, our regularized Laplacian matrix extends the classical regularized Laplacian matrix to multi-layer networks. We establish the consistency property of RDSoS under the multi-layer stochastic block model (MLSBM) and further extend RDSoS and its theoretical results to the degree-corrected version of the MLSBM model. The effectiveness of the proposed methods is evaluated and demonstrated through synthetic and real datasets.

Keywords: Community detection, network analysis, regularized debiased spectral methods, consistency

1. Introduction

Multi-layer (dynamic) networks are extensively collected in various fields like social, biological, and computer sciences, providing a rich and significant framework for describing complex systems characterized by diverse interactions and relationships. These networks are typically represented by edges among nodes in distinct layers (Mucha et al., 2010; Kivelä et al., 2014; Boccaletti et al., 2014). For instance, in social sciences, individuals are connected through various social platforms such as Facebook, Twitter, Instagram, and emails, forming a multi-layer social network with each layer denoting a distinct type of social relationship, ranging from friendships to professional connections (Ansari et al., 2011; Oselio et al., 2014). Similarly, in biological sciences, proteins engage in interactions through various biological processes or different stages of development, resulting in a multi-layer protein-protein interaction network where different layers signify different types of biological interactions or different times (Bakken et al., 2016;

*Corresponding author.

Email address: qinghuan@u.nus.edu; qinghuan@cqut.edu.cn; qinghuan07131995@163.com (Huan Qing)

Zhang & Cao, 2017; Lei & Lin, 2023). Another tangible example is transportation networks, where different modes of transportation, such as buses, trains, and subways, can be depicted as separate layers interconnected by transfer stations or stops.

Community detection is a fundamental problem in analyzing multi-layer networks. It involves finding groups (blocks/communities/clusters) of nodes that are densely connected within the group, but sparsely connected to nodes in other groups (Newman & Girvan, 2004; Jin et al., 2021; Huang et al., 2021). It can reveal underlying structural patterns and functional modules within networks, providing valuable insights into the organization and dynamics of complex systems (Fortunato, 2010; Fortunato & Hric, 2016). For instance, communities may stand for groups of individuals who share common interests or behaviors in social networks, while in biological networks, they may correspond to functional modules. Multi-layer networks have more edges than single-layer (static) networks, thus providing more community information (Paul & Chen, 2020; Lei & Lin, 2023). This work studies the community detection problem in multi-layer networks where layers share common nodes but have no cross-layer connections.

The multi-layer stochastic block model (MLSBM) is a powerful model in describing the hidden community structure of multi-layer networks. This model extends the classical stochastic block model (SBM) (Holland et al., 1983) from static networks to multi-layer networks. Under the MLSBM, nodes are assumed to belong to latent communities, and edges among nodes are generated by specific probabilistic rules that may vary across different layers. Several methods have been developed to discover nodes' communities under the MLSBM, and their theoretical consistencies have been thoroughly investigated. For instance, (Han et al., 2015) studied the asymptotic properties of a spectral method and a maximum-likelihood method when $T \rightarrow \infty$ and n is fixed under the MLSBM, where T denotes the number of layers and n represents the number of vertices. (Paul & Chen, 2020) established the theoretical consistency of spectral and matrix factorization approaches when $T \rightarrow \infty$ and $n \rightarrow \infty$ under the MLSBM model. (Lei et al., 2020) proposed a least squares estimation approach to fit the MLSBM and established its theoretical analysis when $T \rightarrow \infty$ and $n \rightarrow \infty$. Recently, (Lei & Lin, 2023) developed an efficient spectral method via the debiased sum of squared adjacency matrices and studied its consistency as $T \rightarrow \infty$ and $n \rightarrow \infty$ within the framework of the MLSBM. However, a notable limitation of the MLSBM is that it does not consider the variety of nodes' degrees, a prevalent characteristic of real-world networks. The multi-layer degree-corrected stochastic block model (MLDCSBM) (Qing, 2024) has been introduced to overcome MLSBM's limitation. MLDCSBM permits nodes within the identical group to exhibit varying expected degrees and extends the popular degree-corrected stochastic block model (DCSBM) (Karrer & Newman, 2011) from static networks to multi-layer networks. A debiased spectral clustering method with theoretical guarantees is developed to fit MLDCSBM in (Qing, 2024).

In single-layer networks, using the regularized Laplacian matrix $E_\tau^{-\frac{1}{2}} A E_\tau^{-\frac{1}{2}}$ (or $E_\tau^{-\frac{1}{2}} (A + \tau J) E_\tau^{-\frac{1}{2}}$) to design spec-

tral methods has been shown great potential in handling sparse networks (Qin & Rohe, 2013; Joseph & Yu, 2016; Cucuringu et al., 2021) under the SBM and the DCSBM. Here, A denotes the adjacency matrix of a static network, $E_\tau = \tau I + E$ for $\tau \geq 0$, E is a diagonal matrix containing nodes' degrees, J denotes a matrix with all elements being 1, and I represents the identity matrix. The classical regularized Laplacian matrix incorporates a regularization term τ that helps mitigate the impact of noise and sparsity, ultimately enhancing performance in community detection. However, a critical scientific question remains: how can we extend the idea of regularized spectral clustering in static networks to dynamic networks for community detection? Despite the progress made in spectral methods for multi-layer networks under the MLSBM and the MLDCSBM (Han et al., 2015; Paul & Chen, 2020; Lei & Lin, 2023; Qing, 2024), methods using the regularized Laplacian matrix have not been proposed. This gap in the literature motivates the present study, which aims to develop novel methods for discovering nodes' communities in multi-layer networks that harnesses the strengths of regularized spectral clustering.

The key contributions of this work are enumerated below:

1. By applying regularization to the debiased sum of squared adjacency matrices introduced in (Lei & Lin, 2023), we propose a novel regularized Laplacian matrix, denoted as L_τ in Equation (4). This matrix extends the concept of the classical regularized Laplacian matrix to multi-layer networks, incorporating the advantages of the debiased spectral clustering presented in (Lei & Lin, 2023).
2. Leveraging the proposed regularized Laplacian matrix, we develop a new method, termed regularized debiased sum of squared adjacency matrices (RDSoS), for detecting communities in multi-layer networks under the MLSBM. RDSoS identifies communities through applying the K-means algorithm to an eigenvector matrix constructed from the leading eigenvectors of our regularized Laplacian matrix L_τ . Additionally, we propose a degree-corrected RDSoS (DC-RDSoS) method for detecting communities within the MLDCSBM. DC-RDSoS is an enhanced version of RDSoS tailored for multi-layer networks where nodes exhibit varying degrees.
3. We conduct a rigorous analysis of the consistency of RDSoS and DC-RDSoS as $T \rightarrow \infty$ and $n \rightarrow \infty$ under the MLSBM and MLDCSBM, respectively. Our theoretical findings suggest that a moderate value of the regularization parameter τ is preferable.
4. We conduct both numerical and empirical studies to show that our proposed methods achieve at least competitive performance when compared to the current state-of-the-art methods.

Notation. The set $\{1, 2, \dots, m\}$ is denoted by $[m]$. For any matrix M , M' represents its transpose, $M(i, :)$ denotes its i -th row, $\|M\|_F$ denotes the Frobenius norm, $\|M\|$ represents the spectral norm, $\|M\|_1$ is the l_1 norm, $\lambda_m(M)$ denotes the m -th largest eigenvalue of M in terms of magnitude, and $\text{rank}(M)$ means the rank of M . The notations $\mathbb{P}(\cdot)$ and $\mathbb{E}(\cdot)$ are employed to denote the probability and the expectation, respectively.

2. Multi-layer stochastic block model

This part introduces the multi-layer stochastic block model, our first regularized debiased spectral method, and its theoretical properties. We consider the following definition for the model.

Definition 1. (MLSBM) Consider a multi-layer network with n common nodes and T layers. Let the $n \times n$ symmetric matrix A_l be the adjacency matrix of the l -th layer network for $l \in [T]$, where $A_l(i, j) = 1$ if there is an edge between nodes i and j and 0 otherwise for all nodes, i.e., we consider undirected unweighted networks in this paper. Assume that all nodes are partitioned into K communities $\{C_k\}_{k=1}^K$, where we assume that K is known in this work. Let $Z \in \{0, 1\}^{n \times K}$, where $Z(i, k) = 1$ if node i belongs to the k -th community C_k and 0 otherwise for $i \in [n], k \in [K]$. Suppose that these communities are disjoint and there is no empty community, ensuring $\text{rank}(Z) = K$. Let the n -by-1 vector ℓ record nodes' community information such that its i -th entry is k if $Z(i, k) = 1$ for $i \in [n], k \in [K]$. For $l \in [T]$, let the $K \times K$ symmetric matrix B_l be the l -th connectivity matrix such that all entries of B_l locate in $[0, 1]$. Given $(Z, \{B_l\}_{l=1}^T)$, the multi-layer stochastic block model (MLSBM) assumes that for $i \in [n], j \in [n], l \in [T]$, each entry of A_l is generated independently as

$$A_l(i, j) = A_l(j, i) \sim \text{Bernoulli}(B_l(\ell(i), \ell(j))). \quad (1)$$

The MLSBM becomes the classical SBM when only one layer, i.e., $T = 1$. Define $\Omega_l = ZB_lZ'$ for $l \in [T]$. We have

$$\mathbb{E}(A_l) = \Omega_l, \quad l \in [T].$$

Thus, Ω_l is the l -th population adjacency matrix for $l \in [T]$. Our algorithm for fitting MLSBM is designed based on further analysis of the structure of $\{\Omega_l\}_{l=1}^T$. Set $\rho = \max_{l \in [T]} \max_{k \in [K], \tilde{k} \in [K]} B_l(k, \tilde{k})$. We see that $\rho \in (0, 1]$. Set $\tilde{B}_l = \frac{B_l}{\rho}$ for $l \in [T]$. We have $\tilde{B}_l = \tilde{B}_l' \in (0, 1]^{K \times K}$ and $\Omega_l = \rho Z \tilde{B}_l Z'$ for $l \in [T]$. Meanwhile, for $i \in [n], j \in [n], l \in [T]$, Equation (1) gives

$$\mathbb{P}(A_l(i, j) = 0) = 1 - \rho \tilde{B}_l(\ell(i), \ell(j)).$$

Thus, the network becomes denser (i.e., more edges are generated) as ρ grows, which implies that ρ governs the network's sparsity. For convenience, call ρ the sparsity parameter. Since real networks are usually sparse, analyzing the capability of an algorithm in multi-layer networks under different levels of sparsity (Lei & Rinaldo, 2015) is important. For convenience, we use "MLSBM parameterized by $\{Z, \rho, \{\tilde{B}_l\}_{l=1}^T\}$ " to denote the MLSBM defined in

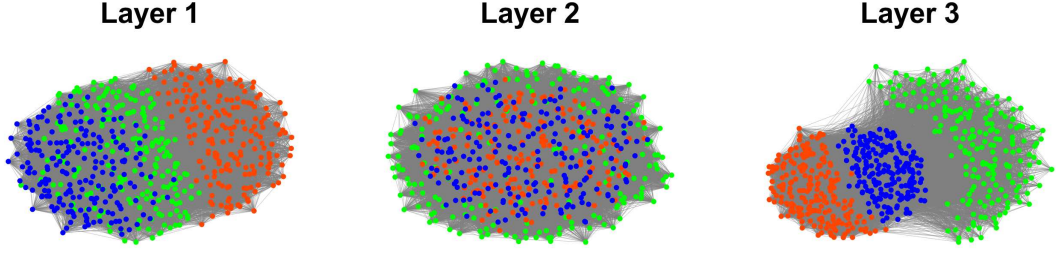


Figure 1: A multi-layer network generated from the MLSBM model with 600 nodes, 3 layers, 3 balanced communities, sparsity parameter $\rho = 0.3$, and B_l 's elements being random values generated from $\text{Unif}(0,1)$. Colors indicate communities. The distinct structure of each layer suggests that nodes exhibit varying connection patterns $\{B_l\}_{l=1}^T$.

Definition 1. Given the model parameters $\{Z, \rho, \{\tilde{B}_l\}_{l=1}^T\}$, the T adjacency matrices $\{A_l\}_{l=1}^T$ can be generated by the MLSBM model through Equation (1). Figure 1 displays a simulated multi-layer network derived from the MLSBM model. Community detection aims to estimate the node label vectors ℓ by leveraging the T adjacency matrices $\{A_l\}_{l=1}^T$. In particular, the objective in Figure 1 is to recognize nodes that share the same color across the three layers, even in the absence of initial color assignments.

For $k \in [K]$, let n_k be the size of the k -th community C_k . Let the superscript c represent a complement set and \mathcal{P}_K denote the set collecting all permutations of $\{1, 2, \dots, K\}$. Set the $n \times 1$ vector $\hat{\ell}$ as an estimated label vector returned by any method (say method \mathcal{M}) when there are K communities. For $k \in [K]$, define \mathcal{E}_k as the k -th estimated community such that node i belongs to \mathcal{E}_k if $\hat{\ell}(i) = k$. To quantify the difference between the true community partitions $\{C_k\}_{k=1}^K$ and the estimated community partitions $\{\mathcal{E}_k\}_{k=1}^K$, we use the metric *Clustering error* defined in Equation (6) of (Joseph & Yu, 2016). The Clustering error can be computed in the following way:

$$\hat{f}_{\mathcal{M}} = \min_{p \in \mathcal{P}_K} \max_{k \in [K]} \frac{|C_k \cap \mathcal{E}_{p(k)}^c| + |C_k^c \cap \mathcal{E}_{p(k)}|}{n_k}, \quad (2)$$

where we use $\hat{f}_{\mathcal{M}}$ to represent the Clustering error of the method \mathcal{M} when the estimated community label $\hat{\ell}$ is returned from \mathcal{M} . To establish the estimation consistency of the proposed methods, we will provide the theoretical upper bounds of their Clustering errors by considering the influence of the model parameters in this work.

2.1. The RDSoS algorithm

Under the MLSBM model, the heuristic of designing an efficient method to detect nodes' communities is to consider the oracle case when the T population adjacency matrices $\{\Omega_l\}_{l=1}^T$ are given. It is expected that a good community detection method should perfectly recover the community partitions in such an oracle case.

Define an $n \times n$ aggregation matrix \mathcal{S} as $\mathcal{S} = \sum_{l \in [T]} \Omega_l^2$, which is the sum of the T squared population adjacency matrices. Define \mathcal{D} as a diagonal matrix with $\mathcal{D}(i, i) = \sum_{j \in [n]} \mathcal{S}(i, j)$ for $i \in [n]$. Set $\mathcal{D}_\tau = \tau I + \mathcal{D}$, where τ is the

nonnegative regularizer. This work introduces a population regularized Laplacian matrix \mathcal{L}_τ as

$$\mathcal{L}_\tau = \mathcal{D}_\tau^{-\frac{1}{2}} \mathcal{S} \mathcal{D}_\tau^{-\frac{1}{2}}. \quad (3)$$

Remark 1. *At first glance, our population regularized Laplacian matrix \mathcal{L}_τ defined in Equation (3) shares a similar form as the population Laplacian matrix considered in (Qin & Rohe, 2013; Joseph & Yu, 2016) because both matrices are computed by regularizing certain matrices. However, there is a huge difference between their definitions: our \mathcal{L}_τ is defined based on the aggregation matrix \mathcal{S} computed from the L population adjacency matrices $\{\Omega_l\}_{l=1}^T$ while the population Laplacian matrix studied in (Qin & Rohe, 2013; Joseph & Yu, 2016) is designed based on a single-layer population adjacency matrix. This difference causes that our population regularized Laplacian matrix \mathcal{L}_τ can be used for discovering communities in multi-layer networks whereas the population Laplacian matrix used in (Qin & Rohe, 2013; Joseph & Yu, 2016) only works for a single-layer network.*

The subsequent lemma demonstrates that the compact eigenvector matrix of the population regularized Laplacian matrix \mathcal{L}_τ can reveal the true communities.

Lemma 1. *Under the MLSBM parameterized by $(Z, \rho, \{\tilde{B}_l\}_{l=1}^T)$. When the rank of the sum of squared connectivity matrices $\sum_{l \in [T]} \tilde{B}_l^2$ is K , let the leading K eigen-decomposition of \mathcal{L}_τ be $U \Sigma U'$, where $U'U = I$ and Σ is a $K \times K$ diagonal matrix. We have: (a) if $\ell(i) = \ell(\bar{i})$ for $i \in [n], \bar{i} \in [n]$, then $U(i, :) = U(\bar{i}, :)$; (b) there exists a matrix X such that $U = ZX$, where X satisfies $\|X(\tilde{k}, :) - X(k, :)\|_F = \sqrt{\frac{1}{n_{\tilde{k}}} + \frac{1}{n_k}}$ for $\tilde{k} \neq k, \tilde{k} \in [K], k \in [K]$.*

By Lemma 1, we see that nodes within the same community have the same respective rows in the $n \times K$ eigenvector matrix U . Thus, employing the K-means algorithm to U can perfectly recover nodes' communities. Based on this observation, we see that if there is a good estimation of the eigenvector matrix U , then running K-means to the estimation eigenvector matrix should return a good estimation of nodes' communities. Recall that the eigenvector matrix U is computed from \mathcal{L}_τ which is designed based on the aggregation matrix \mathcal{S} . Therefore, when $\{A_l\}_{l=1}^T$ are known while their population versions $\{\Omega_l\}_{l=1}^T$ are unavailable in the practical case, as long as we can find a good estimator of the aggregation matrix \mathcal{S} from $\{A_l\}_{l=1}^T$, we can design an efficient method to detect nodes' communities. One may think that $\sum_{l \in [T]} A_l^2$ is a good estimator of the aggregation matrix \mathcal{S} since $\mathbb{E}(A_l) = \Omega_l$ for $l \in [T]$. However, as analyzed in (Lei & Lin, 2023), $\sum_{l \in [T]} A_l^2$ is a biased estimation of \mathcal{S} . Instead, $S := \sum_{l \in [T]} (A_l^2 - D_l)$ is a debiased (bias-adjusted) estimator of \mathcal{S} , where $D_l(i, i) = \sum_{j \in [n]} A_l(i, j)$ and $D_l(i, \bar{i}) = 0$ for $i \in [n], \bar{i} \neq i, \bar{i} \in [n], l \in [T]$. S is known as the debiased sum of squared adjacency matrices. Thus, when we design a community detection method, S

should be used instead of $\sum_{l \in [T]} A_l^2$. We are ready to define our regularized Laplacian matrix L_τ :

$$L_\tau = D_\tau^{-\frac{1}{2}} S D_\tau^{-\frac{1}{2}}, \quad (4)$$

where $D_\tau = D + \tau I$ for $\tau \geq 0$ and D is a diagonal matrix with $D(i, i) = \sum_{j \in [n]} S(i, j)$ for $i \in [n]$. Note that D_l differs a lot from D as D_l is the degree matrix of A_l for $l \in [T]$ while D can be seen as the degree matrix of S .

Remark 2. *Similar to Remark 1, though our regularized Laplacian matrix L_τ defined in Equation (4) shares a similar form as the regularized Laplacian matrix studied in (Qin & Rohe, 2013; Joseph & Yu, 2016), they have a huge difference: our regularized Laplacian matrix L_τ is defined using the debiased sum of squared adjacency matrices S , causing that one can design community detection methods for multi-layer networks using our L_τ . In contrast, the one used in (Qin & Rohe, 2013; Joseph & Yu, 2016) is based on a single-layer adjacency matrix and can only be used for single-layer networks.*

Let $\hat{U} \hat{\Sigma} \hat{U}'$ be the leading K eigen-decomposition of L_τ such that $\hat{U}' \hat{U} = I$ and $\hat{\Sigma}(k, k) = \lambda_k(L_\tau)$ of the $K \times K$ diagonal matrix $\hat{\Sigma}$ for $k \in [K]$. Because S is a good estimator of \mathcal{S} , we believe that \hat{U} can be considered a good approximation of U . Therefore, running K-means to \hat{U} with K communities can provide a satisfactory estimation of nodes' communities. The above analysis is summarized by our first algorithm, called “regularized debiased sum of squared adjacency matrices” (RDSoS, Algorithm 1). Our RDSoS is a regularized debiased spectral clustering method because it is designed by clustering the eigenvector matrix of our regularized Laplacian matrix L_τ calculated via Equation (4).

The RDSoS method exhibits the following complexities for its steps: the complexities of Steps 1-5 are $O(Tn^3)$, $O(n^2)$, $O(n^3)$, $O(Kn^2)$, and $O(KnI_{ter})$, respectively, where I_{ter} represents K-means' iteration number, which we have fixed at 100 in this paper. In this work, K is set such that $K \ll n$. Thus, RDSoS's complexity is $O(Tn^3)$.

Algorithm 1 RDSoS

Require: $\{A_l\}_{l=1}^T$, K , and τ .

Ensure: $\hat{\ell}$.

- 1: Compute $S = \sum_{l \in [T]} (A_l^2 - D_l)$.
 - 2: Compute the diagonal matrix D by $D(i, i) = \sum_{j \in [n]} S(i, j)$ for $i \in [n]$.
 - 3: Compute $L_\tau = D_\tau^{-\frac{1}{2}} S D_\tau^{-\frac{1}{2}}$, where $D_\tau = \tau I + D$ (a default value of τ is $\frac{\sum_{i \in [n]} D(i, i)}{n}$).
 - 4: Obtain $\hat{U} \hat{\Sigma} \hat{U}'$, the leading K eigen-decomposition of L_τ .
 - 5: Run the K-means algorithm to \hat{U} with K clusters to obtain the estimated node labels $\hat{\ell}$.
-

2.2. Consistency of RDSoS in MLSBM

This subsection studies RDSoS's estimation consistency within the framework of MLSBM by allowing $n \rightarrow \infty, T \rightarrow \infty$, and $\rho \rightarrow 0$. To establish RDSoS's theoretical guarantees, the next two technical assumptions are needed.

Assumption 1. $\rho^2 n^2 T \geq \log(n + T)$.

Assumption 2. $|\lambda_K(\sum_{l \in [T]} \tilde{B}_l^2)| \geq c_1 T$ for some $c_1 > 0$.

Both assumptions are mild. Assumption 1 only requires $\rho \geq \sqrt{\frac{\log(n+T)}{n^2 T}}$. Thus, the sparsity parameter can be very small (i.e., the multi-layer network can be very sparse) for numerous nodes and/or layers. Assumption 2 only requires that the smallest nonzero eigenvalue in the magnitude of $\sum_{l \in [T]} \tilde{B}_l^2$ has a linear growth with the number of layers T . Note that our Assumptions 1 and 2 are the same as the sparsity requirement in Theorem 1 of (Lei & Lin, 2023) and Assumption 1(b) in (Lei & Lin, 2023), respectively. Set $n_{\max} = \max_{k \in [K]} n_k$ and $\delta_{\max} = \max_{i \in [n]} \mathcal{D}(i, i)$. n_{\min} and δ_{\min} are defined similarly. Theorem 1 below is our main technical result for RDSoS under the MLSBM model.

Theorem 1. *Under the MLSBM parameterized by $(Z, \rho, \{\tilde{B}_l\}_{l=1}^T)$, suppose that Assumptions 1 and 2 are satisfied, we have*

$$\hat{f}_{RDSoS} = \frac{K^2 n_{\max} (\tau + \delta_{\max})^2}{\rho^4 n_{\min}^5 T^2} \left(O\left(\frac{\rho^2 n^2 T \log(n+T)}{(\tau + \delta_{\min})^2}\right) + O\left(\frac{\rho^4 n^2 T^2}{(\tau + \delta_{\min})^2}\right) + O\left(\frac{\rho^4 n^4 T^2 \log^2(n+T)}{(\tau + \delta_{\min})^4}\right) + O\left(\frac{\rho^8 n^4 T^4}{(\tau + \delta_{\min})^4}\right) \right),$$

with probability at least $1 - o(\frac{1}{n+T})$.

The complex form of the bound in Theorem 1 can be simplified by the following analysis.

(Choice of τ) We let $\varrho(\tau) = \frac{K^2 n_{\max} (\tau + \delta_{\max})^2}{\rho^4 n_{\min}^5 T^2} \left(O\left(\frac{\rho^2 n^2 T \log(n+T)}{(\tau + \delta_{\min})^2}\right) + O\left(\frac{\rho^4 n^2 T^2}{(\tau + \delta_{\min})^2}\right) + O\left(\frac{\rho^4 n^4 T^2 \log^2(n+T)}{(\tau + \delta_{\min})^4}\right) + O\left(\frac{\rho^8 n^4 T^4}{(\tau + \delta_{\min})^4}\right) \right)$ be a function of the regularizer τ . On the one hand, Theorem 1 indicates that $\varrho(\tau)$ decreases as τ grows since $\delta_{\min} \leq \delta_{\max}$. This suggests that regularization (the case $\tau > 0$) is theoretically better than non-regularization (the case $\tau = 0$) for the RDSoS algorithm. On the other hand, we know that there is an inverse proportional relationship between $|\lambda_K(L_\tau)|$ and τ since $|\lambda_K(L_\tau)| = |\lambda_K(D_\tau^{-0.5} S D_\tau^{-0.5})| = |\lambda_K(D_\tau^{-1} S)| \geq \lambda_K(D_\tau^{-1}) |\lambda_K(S)| = \frac{|\lambda_K(S)|}{\tau + \max_{i \in [n]} \mathcal{D}(i, i)}$ and $|\lambda_1(L_\tau)| \leq \frac{|\lambda_1(S)|}{\tau + \min_{i \in [n]} \mathcal{D}(i, i)}$. This implies that we can not set the regularization parameter τ too large otherwise the leading K eigenvalues of L_τ may be close to zero, which causes L_τ 's leading K eigenvectors can not provide sufficient information about nodes' communities. Meanwhile, if $0 \leq \tau_1 < \tau_2$, though $\varrho(\tau_1) > \varrho(\tau_2)$, this does not mean that RDSoS- τ_2 strictly outperforms RDSoS- τ_1 since the leading K eigenvectors of L_{τ_2} may contain lesser community information than that of L_{τ_1} , where RDSoS- τ_1 and RDSoS- τ_2 represent the RDSoS algorithm using τ_1 and τ_2 , respectively. Therefore, theoretically speaking, the above analysis suggests that a moderate value of the regularizer τ should be preferred. When $\tau + \delta_{\min} \geq \max(\sqrt{\rho^2 n^2 T \log(n+T)}, \rho^2 n T)$, $\varrho(\tau)$ can be simplified as $\varrho(\tau) = \frac{K^2 n_{\max} (\tau + \delta_{\max})^2}{\rho^4 n_{\min}^5 T^2} \left(O\left(\frac{\rho^2 n^2 T \log(n+T)}{(\tau + \delta_{\min})^2}\right) + O\left(\frac{\rho^4 n^2 T^2}{(\tau + \delta_{\min})^2}\right) \right)$. The form

of $\varrho(\tau)$ can be further simplified as $\varrho(\tau) = \frac{K^2 n_{\max}}{\rho^2 n_{\min}^5 T} (O(n^2 \log(n+T)) + O(\rho^2 n^2 T))$ if τ is set such that $\frac{\tau + \delta_{\max}}{\tau + \delta_{\min}} = O(1)$. Since $0 < \delta_{\min} \leq \mathcal{D}(i, i) \leq \rho^2 n^2 T$, we have $D(i, i) = O(\rho^2 n^2 T)$ with high probability by Lemma 4 for $i \in [n]$. Therefore, setting τ as a moderate value like $\sum_{i \in [n]} D(i, i)/n$ can make $\varrho(t)$ be in its simple form. Sure, larger τ also makes $\varrho(\tau)$ in its simple form.

Setting τ as its default value, we know that

$$\hat{f}_{RDSoS} = O\left(\frac{K^2 n_{\max} n^2 \log(n+T)}{\rho^2 n_{\min}^5 T}\right) + O\left(\frac{K^2 n_{\max} n^2}{n_{\min}^5}\right). \quad (5)$$

By Equation (5), we observe that (a) increasing the sparsity parameter ρ or the number of layers T improves RDSoS's performance; (b) when ρ, T , and n are fixed, decreasing the minimize community size n_{\min} and increasing the number of communities K lead to a harder case for community detection. Furthermore, similar to Assumption 1 of (Lei & Lin, 2023), if we add some conditions on K, n_{\min} , and n_{\max} , the bound in Equation (5) can be further simplified.

Corollary 1. *If K is fixed and the size of each community is balanced, Theorem 1 can be simplified as*

$$\hat{f}_{RDSoS} = O\left(\frac{\log(n+T)}{\rho^2 n^2 T}\right) + O\left(\frac{1}{n^2}\right).$$

The result of Corollary 1 is the same as that of Theorem 1 (Lei & Lin, 2023). This corollary also indicates that when $n \rightarrow \infty$ and/or $T \rightarrow \infty$, RDSoS's Clustering error decreases to 0, implying the estimation consistency of RDSoS.

3. Multi-layer degree-corrected stochastic block model

Under the MLSBM model, akin to the SBM model, nodes belonging to the same community exhibit stochastic equivalence. This equivalence arises because $\mathbb{E}(\sum_{j \in [n]} A_l(i, j)) = \sum_{j \in [n]} \Omega_l(i, j) = Z(i, \cdot) \sum_{j \in [n]} B_l Z'(j, \cdot) \equiv \mathbb{E}(\sum_{j \in [n]} A_l(\bar{i}, j))$ if $\ell(i) = \ell(\bar{i})$ for $i \in [n], \bar{i} \in [n]$, i.e., the expected degrees of two distinct nodes from the same community are identical. However, nodes usually have various degrees in real networks (Karrer & Newman, 2011). Similar to the DCSBM model introduced in (Karrer & Newman, 2011) that extends the SBM model by considering node-specific parameters, the MLDCSBM model introduced in (Qing, 2024) extends the MLSBM model by considering the degree heterogeneity vector $\theta \in (0, 1]^{n \times 1}$ to model networks in which nodes have varying degrees even within the same community. Let Θ be a diagonal matrix with $\Theta(i, i) = \theta(i)$ for $i \in [n]$. We consider the following definition for the MLDCSBM model.

Definition 2. (MLDCSBM) *Let $\{A_l\}_{l=1}^T, Z$, and $\{\tilde{B}_l\}_{l=1}^T$ be the same as that of MLSBM. Given $(Z, \Theta, \{\tilde{B}_l\}_{l=1}^T)$, the MLD-*

CSBM assumes that

$$A_l(i, j) = A_l(j, i) \sim \text{Bernoulli}(\theta(i)\theta(j)\tilde{B}_l(\ell(i), \ell(j))), \quad i \in [n], j \in [n], l \in [T]. \quad (6)$$

For convenience, we use “MLDCSBM parameterized by $\{Z, \Theta, \{\tilde{B}_l\}_{l=1}^T\}$ ” to denote the MLDCSBM in Definition 2. When $T = 1$, MLDCSBM degenerates to the popular DCSBM. When setting $\Theta = \sqrt{\rho}I$ for $\rho \in (0, 1]$, the MLDCSBM model in Definition 2 reduces to the MLSBM model. Without confusion, under the MLDCSBM model, we also let Ω_l be the population adjacency matrix of A_l for $l \in [T]$, $\mathcal{S} := \sum_{l \in [T]} \Omega_l^2$ be the sum of the T squared population adjacency matrices, and $\mathcal{L}_\tau := \mathcal{D}_\tau^{-\frac{1}{2}} \mathcal{S} \mathcal{D}_\tau^{-\frac{1}{2}}$ be the population regularized Laplacian matrix. Under the MLDCSBM model, we have

$$\Omega_l = \Theta Z \tilde{B}_l Z' \Theta, \quad l \in [T].$$

We see that $\mathbb{E}(\sum_{j \in [n]} A_l(i, j)) = \sum_{j \in [n]} \Omega_l(i, j) = \sum_{j \in [n]} \theta(i)\theta(j)Z(i, :)\tilde{B}_l Z'(j, :) = \theta(i)Z(i, :)\sum_{j \in [n]} \theta(j)\tilde{B}_l Z'(j, :)$ for $i \in [n], l \in [T]$ under the MLDCSBM, which implies that vertices from the same group may still have distinct expected degrees if their degree heterogeneity parameters are different. In the next subsection, we introduce a regularized debiased spectral clustering method to estimate nodes’ label information under the MLDCSBM model.

3.1. The DC-RDSoS algorithm

The next lemma functions similarly to Lemma 1 and reveals the structure in \mathcal{L}_τ under the MLDCSBM.

Lemma 2. *Under the MLDCSBM parameterized by $(Z, \Theta, \{\tilde{B}_l\}_{l=1}^T)$, when the rank of the sum of squared connectivity matrices $\sum_{l \in [T]} \tilde{B}_l^2$ is K . Without confusion with the case under the MLSBM, we also let $U \Sigma U'$ be \mathcal{L}_τ ’s leading K eigen-decomposition. Let $U_*(i, :) = \frac{U(i, :)}{\|U(i, :)\|_F}$ for $i \in [n]$. Then, we have: (a) if $\ell(i) = \ell(\bar{i})$ for $i \in [n], \bar{i} \in [n]$, $U_*(i, :) = U_*(\bar{i}, :)$; (b) $U_* = ZY$ with Y satisfying $\|Y(\tilde{k}, :) - Y(k, :)\|_F = \sqrt{2}$ for $\tilde{k} \neq k, \tilde{k} \in [K], k \in [K]$.*

Lemma 2 says that there may exist more than K distinct rows in the eigenvector matrix U under the MLDCSBM due to the effect of the degree heterogeneity parameters Θ . Therefore, applying K-means to U may not exactly recover nodes’ communities under the MLDCSBM. Instead, U_* , U ’s row-normalized version, has exactly K different rows, and employing K-means to it can perfectly recover nodes’ communities. Define S and L_τ the same as that of Algorithm 1. Set \hat{U}_* as \hat{U} ’s row-normalized version such that $\hat{U}_*(i, :) = \frac{\hat{U}(i, :)}{\|\hat{U}(i, :)\|_F}$ for $i \in [n]$. We see that \hat{U}_* is a good approximation of U_* and applying K-means to it should return good estimations of nodes’ community partitions. Our second algorithm, called “Degree-corrected regularized debiased sum of squared adjacency matrices” (DC-RDSoS,

Algorithm 2) summarizes the above analysis. Sure, our DC-RDSoS is also a regularized debiased spectral clustering method. Moreover, the complexity cost of the DC-RDSoS algorithm is identical to that of RDSoS.

Algorithm 2 DC-RDSoS

Require: $\{A_l\}_{l=1}^T$, K , and τ .

Ensure: $\hat{\ell}$.

- 1: Compute \hat{U} using the steps 1-4 of Algorithm 1.
 - 2: Compute \hat{U}_* .
 - 3: Run K-means to \hat{U}_* with K clusters to get $\hat{\ell}$.
-

3.2. Consistency of DC-RDSoS in MLDCSBM

Our DC-RDSoS method also holds consistent estimation under the MLDCSBM model. Set $\theta_{\min} = \min_{i \in [n]} \theta(i)$ and $\theta_{\max} = \max_{i \in [n]} \theta(i)$. Assumption 3 below functions similar to Assumption 1.

Assumption 3. $\theta_{\max} \|\theta\|_1 \|\theta\|_F^2 T \geq \log(n + T)$.

When the MLDCSBM reduces to the MLSBM by setting $\Theta = \sqrt{\rho}I$, we see that Assumption 3 degenerates to Assumption 1.

The following lemma bounds $\|L_\tau - \mathcal{L}_\tau\|$ under the MLDCSBM and it shows that L_τ is close to its population version \mathcal{L}_τ in spectral norm. In proving Theorem 1, the bound of $\|L_\tau - \mathcal{L}_\tau\|$ under the MLSBM is also required. This bound can be immediately obtained from Lemma 3 below by simply setting $\theta(i) = \sqrt{\rho}$ for $i \in [n]$.

Lemma 3. *Under the MLDCSBM parameterized by $(Z, \Theta, \{\tilde{B}_l\}_{l=1}^T)$. If Assumption 3 is satisfied, we have*

$$\|L_\tau - \mathcal{L}_\tau\| = O\left(\frac{\sqrt{\theta_{\max} \|\theta\|_1 \|\theta\|_F^2 T \log(n + T)}}{\tau + \delta_{\min}}\right) + O\left(\frac{\theta_{\max}^2 \|\theta\|_F^2 T}{\tau + \delta_{\min}}\right) + O\left(\frac{\theta_{\max} \|\theta\|_1 \|\theta\|_F^2 T \log(n + T)}{(\tau + \delta_{\min})^2}\right) + O\left(\frac{\theta_{\max}^4 \|\theta\|_F^4 T^2}{(\tau + \delta_{\min})^2}\right),$$

with probability at least $1 - o(\frac{1}{n+T})$.

Theorem 2 quantifies DC-RDSoS's clustering performance under the MLDCSBM model.

Theorem 2. *Under the MLDCSBM parameterized by $(Z, \Theta, \{\tilde{B}_l\}_{l=1}^T)$, suppose that Assumptions 2 and 3 are satisfied, we have*

$$\begin{aligned} \hat{f}_{DC-RDSoS} &= \frac{\theta_{\max}^2 (\tau + \delta_{\max})^3 K^2 n_{\max}}{\theta_{\min}^{10} (\tau + \delta_{\min}) n_{\min}^5 T^2} \left(O\left(\frac{\theta_{\max} \|\theta\|_1 \|\theta\|_F^2 T \log(n + T)}{(\tau + \delta_{\min})^2}\right) + O\left(\frac{\theta_{\max}^4 \|\theta\|_F^4 T^2}{(\tau + \delta_{\min})^2}\right) + O\left(\frac{\theta_{\max}^2 \|\theta\|_1 \|\theta\|_F^4 T^2 \log^2(n + T)}{(\tau + \delta_{\min})^4}\right) \right) \\ &\quad + O\left(\frac{\theta_{\max}^8 \|\theta\|_F^8 T^4}{(\tau + \delta_{\min})^4}\right), \end{aligned}$$

with probability at least $1 - o(\frac{1}{n+T})$.

Similar to the analysis after Theorem 1, a moderate value of τ is preferred for DC-RDSoS. Setting τ as its default value $\frac{\sum_{i \in [n]} D(i,i)}{n}$ gives

$$\hat{f}_{DC-RDSoS} = \frac{\theta_{\max}^2 K^2 n_{\max}}{\theta_{\min}^{10} n_{\min}^5 T^2} (O(\theta_{\max} \|\theta\|_1 \|\theta\|_F^2 T \log(n+T)) + O(\theta_{\max}^4 \|\theta\|_F^4 T^2)). \quad (7)$$

By setting $\Theta = \sqrt{\rho}I$, MLDCSBM becomes MLSBM and we see that the theoretical bound of $\hat{f}_{DC-RDSoS}$ in Equation (7) is consistent with that of Equation (5). The next corollary functions similar to Corollary 1.

Corollary 2. *If $K = O(1)$, $\frac{n_{\min}}{n_{\max}} = O(1)$, and $\theta(i) = O(\sqrt{\rho})$ for any $\rho \in (0, 1]$ for $i \in [n]$, Theorem 2 can be simplified as*

$$\hat{f}_{DC-RDSoS} = O\left(\frac{\log(n+T)}{\rho^2 n^2 T}\right) + O\left(\frac{1}{n^2}\right).$$

4. Simulations

This section conducts simulation studies to investigate the performance of our RDSoS and DC-RDSoS by comparing them with the following methods:

- **SoS-Debias:** this method is proposed by (Lei & Lin, 2023) and it is designed by substituting S for L_τ in Algorithm 1, i.e., it does not consider regularized Laplacian matrix. Estimation consistency of SoS-Debias under the MLSBM is provided in (Lei & Lin, 2023).
- **NDSoS:** this algorithm is introduced in (Qing, 2024) and it is designed by substituting S for L_τ in Algorithm 2. Its theoretical convergence is analyzed in (Qing, 2024) under the MLDCSBM.
- **MASE:** it is a spectral embedding algorithm proposed by (Arroyo et al., 2021) to estimate nodes' communities.

Remark 3. *In this work, we do not consider other baseline methods mentioned in (Arroyo et al., 2021; Lei & Lin, 2023; Qing, 2024) for comparison, as the primary algorithms proposed in these works typically exhibit superior performance compared to these baseline methods, as evidenced by their numerical studies. Meanwhile, we design four new algorithms: RSum, RSoS, DC-RSum, and DC-RSoS. These methods are derived by substituting $A_{\text{sum}} = \sum_{l \in [T]} A_l$ for S in Algorithm 1, substituting $\tilde{S} = \sum_{l \in [T]} A_l^2$ for S in Algorithm 1, substituting A_{sum} for S in Algorithm 2, and substituting \tilde{S} for S in Algorithm 2, respectively. Utilizing a proof analogous to that of Theorems 1 and 2, we can establish the estimation consistencies of RSum (RSoS) and DC-RSum (DC-RSoS) under the MLSBM and the MLDCSBM, respectively. Furthermore, adapting a similar theoretical analysis from (Qing, 2024), we can demonstrate that our RDSoS generally outperforms RSum and RSoS in the MLSBM, and our DC-RDSoS generally outperforms DC-RSum and DC-RSoS in the MLDCSBM. Detailed proofs are omitted for brevity. Consistent with numerical results in*

(Lei & Lin, 2023; Qing, 2024), debiased spectral clustering methods typically exhibit lower error rates than spectral methods using A_{sum} or \tilde{S} . Hence, we do not consider these four methods in our experimental studies in this paper.

For simulated datasets with knowing the true node community information ℓ , the performance of the above methods is evaluated using the following measures: Clustering error (Joseph & Yu, 2016), Hamming error (Jin, 2015), ARI (Hubert & Arabie, 1985), and NMI (Strehl & Ghosh, 2002). For Clustering error and Hamming error, lower values indicate better performance, while for ARI and NMI, higher values indicate better performance.

For all simulation studies, we set $K = 3$ and generate three communities with imbalanced sizes: $n_1 = \frac{n}{2}$, $n_2 = \frac{n}{5}$, and $n_3 = \frac{3n}{10}$, where n is a multiple of 10. First, let each entry of \tilde{B}_l be generated from $\text{Unif}(0,1)$. Then update \tilde{B}_l by letting it be $\frac{\tilde{B}_l + \tilde{B}_l'}{2}$ to make it symmetric for $l \in [T]$. For the MLDCSBM, we set $\theta(i) = \sqrt{\rho} \frac{\ell(i)}{K} \text{rand}(1)$ for $i \in [n]$, where $\text{rand}(1) \sim \text{Unif}(0, 1)$. Thus, in simulated multi-layer networks generated from the MLDCSBM, each node may have a different heterogeneity parameter. Each simulation study considers two cases: the MLSBM case and the MLDCSBM case, where $\Omega_l = \rho Z \tilde{B}_l Z'$ under the MLSBM case and $\Omega_l = \rho \Theta Z \tilde{B}_l Z' \Theta$ under the MLDCSBM case for all $l \in [T]$. For each simulation study, n , T , and ρ are set independently. Finally, 50 independent replicates are generated in every simulation setting, and we report the mean outcomes across these 50 repetitions for each metric.

Simulation study 1: varying the number of nodes n . For the MLSBM case, we set $\rho = 0.04$, $T = 10$, and vary n in $\{200, 400, \dots, 1000\}$. For the MLDCSBM case, we set $\rho = 0.16$, $T = 5$, and vary n in $\{1000, 2000, \dots, 5000\}$. Results shown in Figure 2 say that (a) all algorithms behave better when n grows, except for MASE, whose Clustering Error and Hamming Error almost do not decrease in the MLDCSBM case; (b) our RDSoS and DC-RDSoS slightly outperform SoS-Debias and NDSoS, and these four methods outperform MASE in the MLSBM case; (c) our RDSoS and DC-RDSoS significantly outperform their competitors in the MLDCSBM case.

Simulation study 2: varying the number of layers T . For the MLSBM case, we set $n = 200$ and $\rho = 0.04$. For the MLDCSBM case, we set $n = 500$ and $\rho = 0.16$. In both cases, we vary T in $\{10, 20, \dots, 100\}$. From Figure 3, we observe that (a) as the number of layers grows, all approaches enjoy better performance; (b) the proposed RDSoS and DC-RDSoS methods outperform their competitors in this simulation.

Simulation study 3: varying the sparsity parameter ρ . For the MLSBM case, we set $n = 200$ and $T = 10$. For the MLDCSBM case, we set $n = 500$ and $T = 50$. In both cases, we vary ρ in $\{0.05^2, 0.1^2, 0.15^2, \dots, 0.8^2\}$. According to Figure 4, we observe that (a) each method behaves better in the task of estimating ℓ when we increase the sparsity parameter ρ , except when ρ is too small; (b) our RDSoS and DC-RDSoS have similar performances to SoS-Debias and NDSoS in the MLSBM case; (c) our proposed methods significantly outperform SoS-Debias, NDSoS, and MASE in the MLDCSBM case.

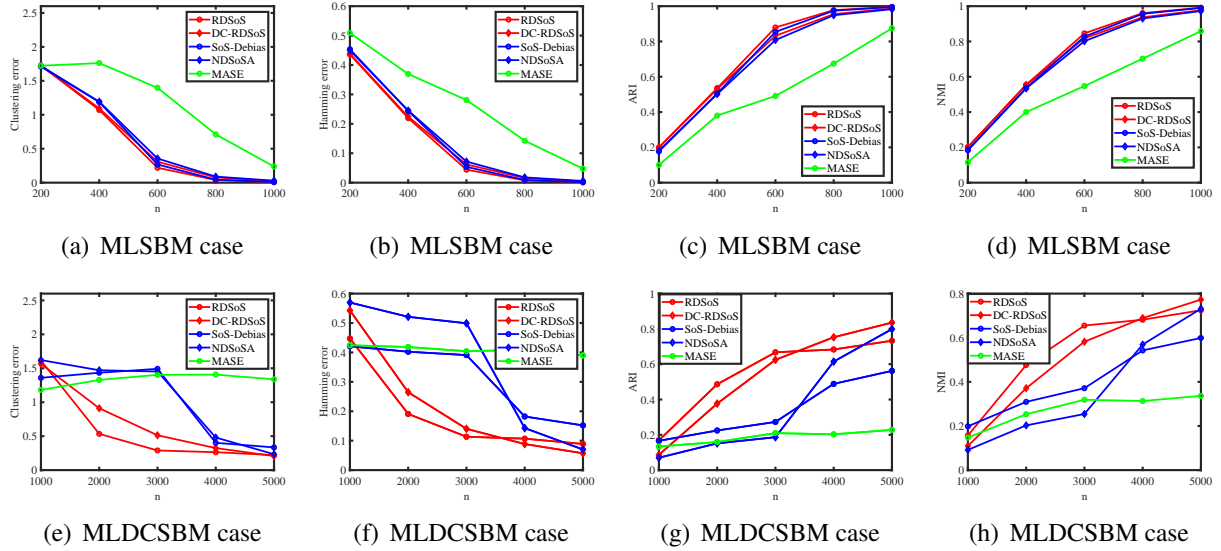


Figure 2: Performances of different methods in Simulation 1.

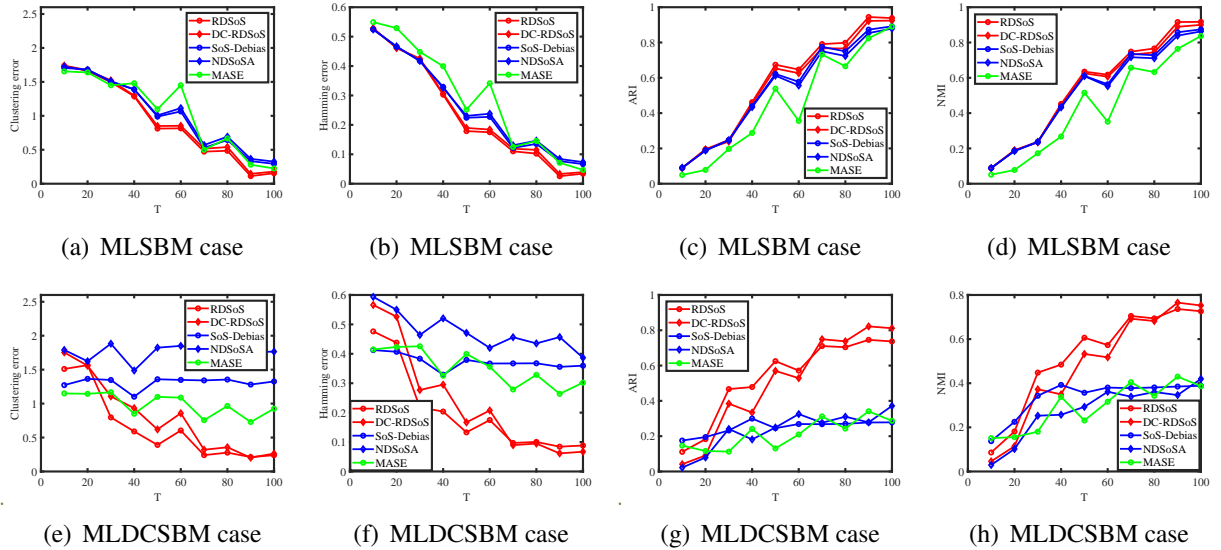


Figure 3: Performances of different methods in Simulation 2.

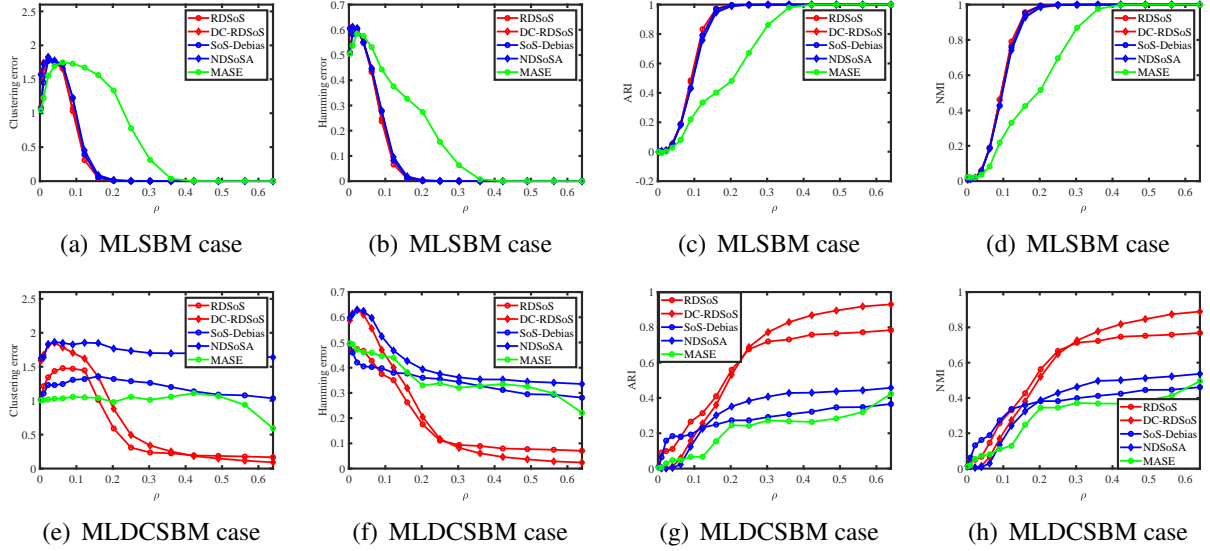


Figure 4: Performances of different methods in Simulation 3.

5. Real-world multi-layer networks

We evaluate the capability of the proposed RDSoS and DC-RDSoS and their competitors in real-world multi-layer networks in this part. Four real datasets are considered, and their main information is reported in Table 1.

In real-world data, the ground truth community labels and the number of communities are often unknown. Therefore, the four metrics considered in Section 4 are no longer applicable. Instead, we utilize the multi-normalized average (MNavrg) modularity defined in Equation (3.1) Paul & Chen (2021) to measure the quality of community partitions for real data when the true node labels are unavailable. Given any community detection method \mathcal{M} applied to a real multi-layer network with T adjacency matrices $\{A_l\}_{l=1}^T$ and assuming k communities, let $\hat{\ell}_{\mathcal{M},k}$ denote the estimated node labels returned by \mathcal{M} . For $l \in [T]$, let d_l be an $n \times 1$ vector with $d_l(i) = D_l(i, i)$ for $i \in [n]$. For $l \in [T]$, set $e_l = \sum_{i \in [n]} d(i)/2$. Set $\mathbb{1}$ as the indicator function. The MNavrg metric can be calculated as follows:

$$Q_{MNavrg}(\mathcal{M}, k) = \frac{1}{T} \sum_{l \in [T]} \sum_{i \in [n], j \in [n]} \frac{1}{2e_l} (A_l(i, j) - \frac{d_l(i)d_l(j)}{2e_l}) \mathbb{1}(\hat{\ell}_{\mathcal{M},k}(i) = \hat{\ell}_{\mathcal{M},k}(j)).$$

The value $Q_{MNavrg}(\mathcal{M}, k)$ ranges in $[0, 1]$ and can be interpreted as the average of the Newman-Girvan modularity Newman & Girvan (2004) across all layers. Similar to the Newman-Girvan modularity, a higher value of MNavrg indicates better quality of the estimated communities. For real multi-layer networks without knowing the true number of communities K , suppose that K may be one of $\{1, 2, \dots, K_C\}$, where we set K_C to be 20 in this paper, based on the observation that K is not excessively large for real multi-layer networks. Thus, for method \mathcal{M} , we obtain K_C MNavrg

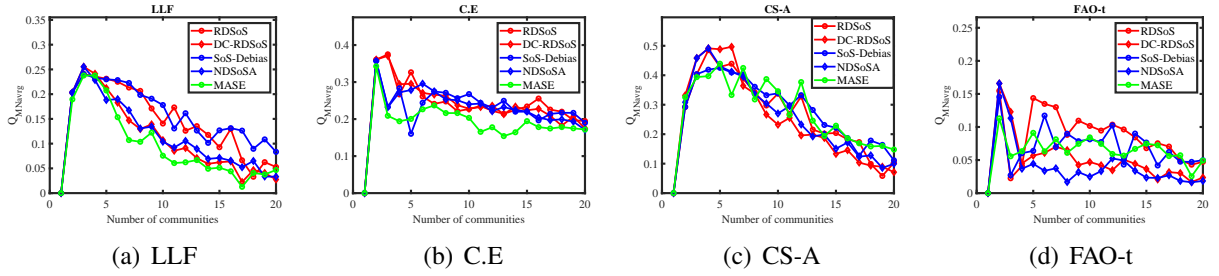


Figure 5: Q_{MNavrg} against the possible number of communities k for the four real multi-layer networks listed in Table 1.

values $\{Q_{MNavrg}(\mathcal{M}, k)\}_{k=1}^{K_C}$. In line with [Nepusz et al. \(2008\)](#); [Qing & Wang \(2023a\)](#), we estimate K by maximizing $MNavrg$, denoted as $K_M = \arg \max_{k \in [K_C]} Q_{MNavrg}(\mathcal{M}, k)$ for method \mathcal{M} . Let $Q_M = Q_{MNavrg}(\mathcal{M}, K_M)$. Considering the five methods: RDSoS, DC-RDSoS, SoS-Debias, NDSoS, and MASE, we obtain five estimates of K for any real multi-layer network \mathcal{N} . These estimates can differ since the methods are distinct. We consider method \mathcal{M} to provide better community partitions if its Q_M is greater than that of its competitors.

Table 1: The four multi-layer networks analyzed in this work.

	Source	Node meaning	Edge meaning	Layer meaning	n	T
Lazega Law Firm (LLF)	Snijders et al. (2006)	Partners	Communication	Advice/Friendship/Co-work	71	3
C.Elegans (C.E)	Chen et al. (2006)	Caenorhabditis elegans	Connectome	Electric/Chemical Monadic/Chemical Polyadic	279	3
CS-Aarhus (CS-A)	Magnani et al. (2013)	Employees	Relationship	Lunch/Facebook/Coauthor/Leisure/Work	61	5
FAO-trade (FAO-t)	De Domenico et al. (2015)	Countries	Import/export relationship	Food products	214	364

Table 2: (K_M, Q_M) for the four real multi-layer networks, with the largest Q_M in bold.

Dataset	RDSoS	DC-RDSoS	SoS-Debias	NDSoS	MASE
LLF	(3,0.2406)	(3,0.2553)	(3,0.2406)	(3,0.2553)	(3,0.2377)
C.E	(3,0.3749)	(3,0.3710)	(2,0.3570)	(2,0.3570)	(2,0.3426)
CS-A	(4,0.4853)	(6,0.4966)	(5,0.4252)	(4,0.4913)	(5,0.4392)
FAO-t	(2,0.1546)	(2,0.1658)	(2,0.1456)	(2,0.1658)	(2,0.1131)

Figure 5 illustrates the relationship between Q_{MNavrg} and the possible number of communities for every network. According to the results of this figure, we can determine the k that maximizes Q_{MNavrg} for each method in each dataset. Table 2 presents the specific (K_M, Q_M) values for each method across all real datasets. Our observations are as follows:

- Our RDSoS and DC-RDSoS methods exhibit competitive performance, often matching or exceeding the best results of their competitors. Specifically, DC-RDSoS and NDSoS outperform the other three methods for LLF and FAO-t, respectively. RDSoS and DC-RDSoS achieve the best community partitions for C.E and CS-A, respectively.
- For LLF and FAO-t, the number of communities returned by all methods is 3 and 2, respectively. For C.E, the

value of K should be set to 3, as RDSoS achieves the maximum value of MNavrg at $k = 3$. Similarly, for CS-A, the value of K should be set to 6, as DC-RDSoS achieves the maximum value of MNavrg at $k = 6$.

- The community structure of CS-A is more pronounced than that of LLF, C.E, and FAO-t, as evidenced by the highest maximum MNavrg value of 0.4966 for CS-A in Table 2. By contrast, FAO-t’s community structure is the least pronounced, as its maximum MNavrg value is 0.1658, even smaller than the minimum MNavrg value of the other datasets.

In Figure 6, we present the adjacency matrices of these real-world multi-layer networks, where the nodes are rearranged based on the estimated community partitions. From this figure, it is evident that nodes within the same community (indicated by the square section in the diagonal part of each adjacency matrix) exhibit a higher number of connections compared to nodes across different communities, suggesting that these multi-layer networks are assortative (Newman, 2002). For visualization purposes, we present the estimated community structure for each multi-layer network in Figure 7.

6. Discussion

This paper introduces a novel regularized Laplacian matrix L_τ to extend the concept of the classical regularized Laplacian matrix, typically used for community detection in single-layer networks, to multi-layer networks. Based on L_τ , two novel regularized debiased spectral clustering methods, RDSoS and DC-RDSoS, are developed. The consistency results of both methods are established under the MLSBM and the MLDCSBM, respectively. Under mild conditions, the theoretical results of both methods match those of Theorem 1 in (Lei & Lin, 2023) in the MLSBM. Extensive experimental results demonstrate the satisfactory empirical performance of both methods.

The idea presented in this paper holds potential for several promising avenues of future research. Here, we outline a few of them. Firstly, expanding the concept to multi-layer directed networks modeled by a directed version of the MLSBM (Su et al., 2024) is appealing. Secondly, estimating the number of communities K in the MLSBM and the MLDCSBM using methods with theoretical guarantees is a challenging and meaningful problem. Thirdly, one can design a method that removes the effect of θ by employing the entry-wise ratios idea introduced in (Jin, 2015). Studying the estimation consistency of this method under the MLDCSBM is appealing. Fourthly, if we design our RDSoS and DC-RDSoS using the regularized Laplacian matrix defined as $D_\tau^{-\beta} S D_\tau^{-\beta}$, studying the optimal β under the MLSBM and the MLDCSBM, similar to works in (Ali & Couillet, 2018), is a challenging and appealing task. Lastly, (Deng et al., 2021) studied the strong consistency of graph Laplacians within the SBM framework. As our methods also employ the regularized Laplacian matrix L_τ , studying their strong consistency under the MLSBM and the MLDCSBM for multi-layer networks is a valuable problem.

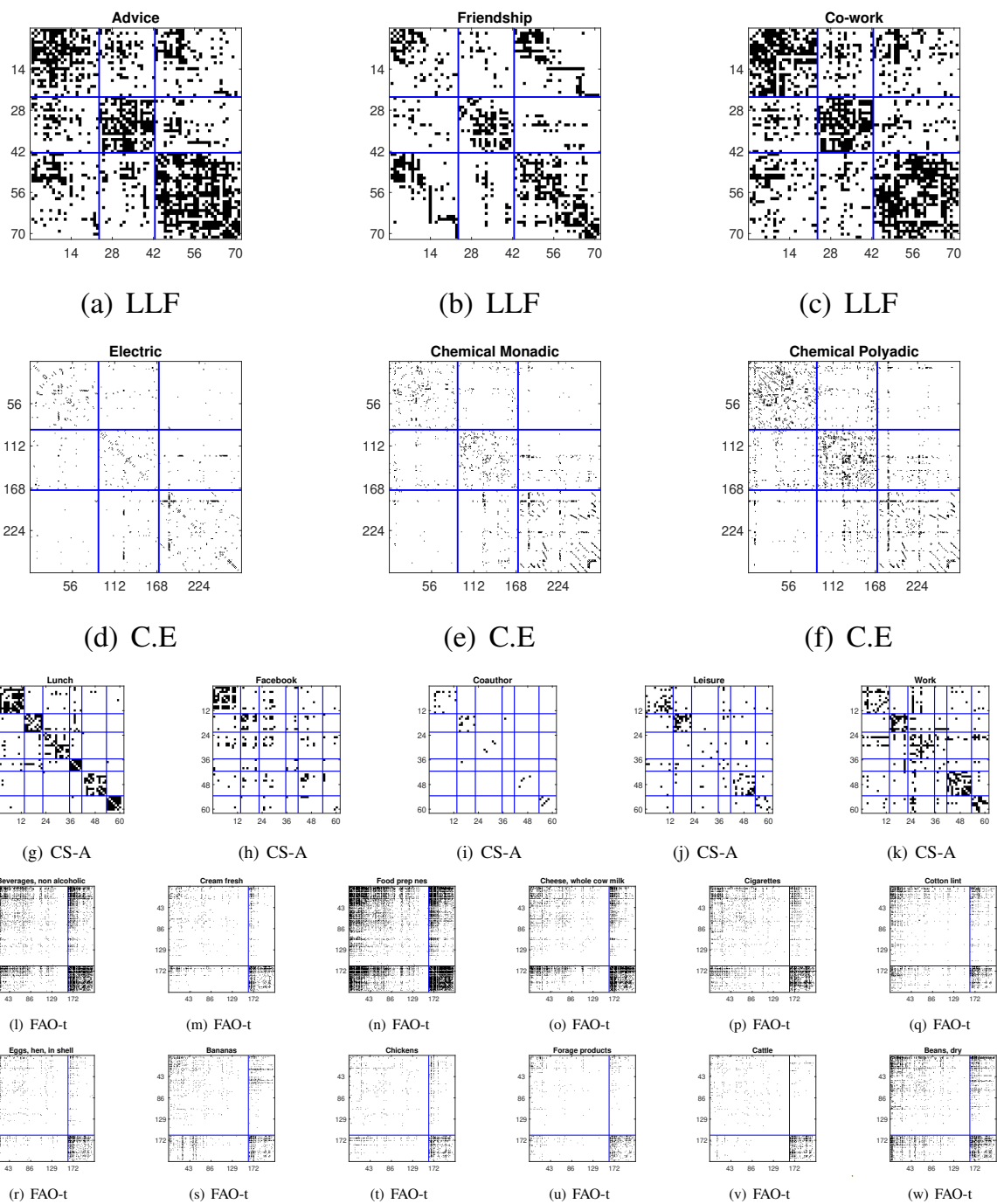


Figure 6: Panels (a)-(c) display the LLF multi-layer network. Panels (d)-(f) display the C.E multi-layer network. Panels (g)-(k) display the CS-A multi-layer network. Panels (l)-(w) display twelve products of FAO-t multi-layer network. The nodes in LLF have been reordered based on the three communities detected by DC-RDSoS. The nodes in C.E have been reordered based on the three communities detected by RDSoS. The nodes in CS-A have been reordered based on the six communities detected by DC-RDSoS. The nodes in FAO-t have been reordered based on the two communities detected by DC-RDSoS. Blue lines represent community partitions.

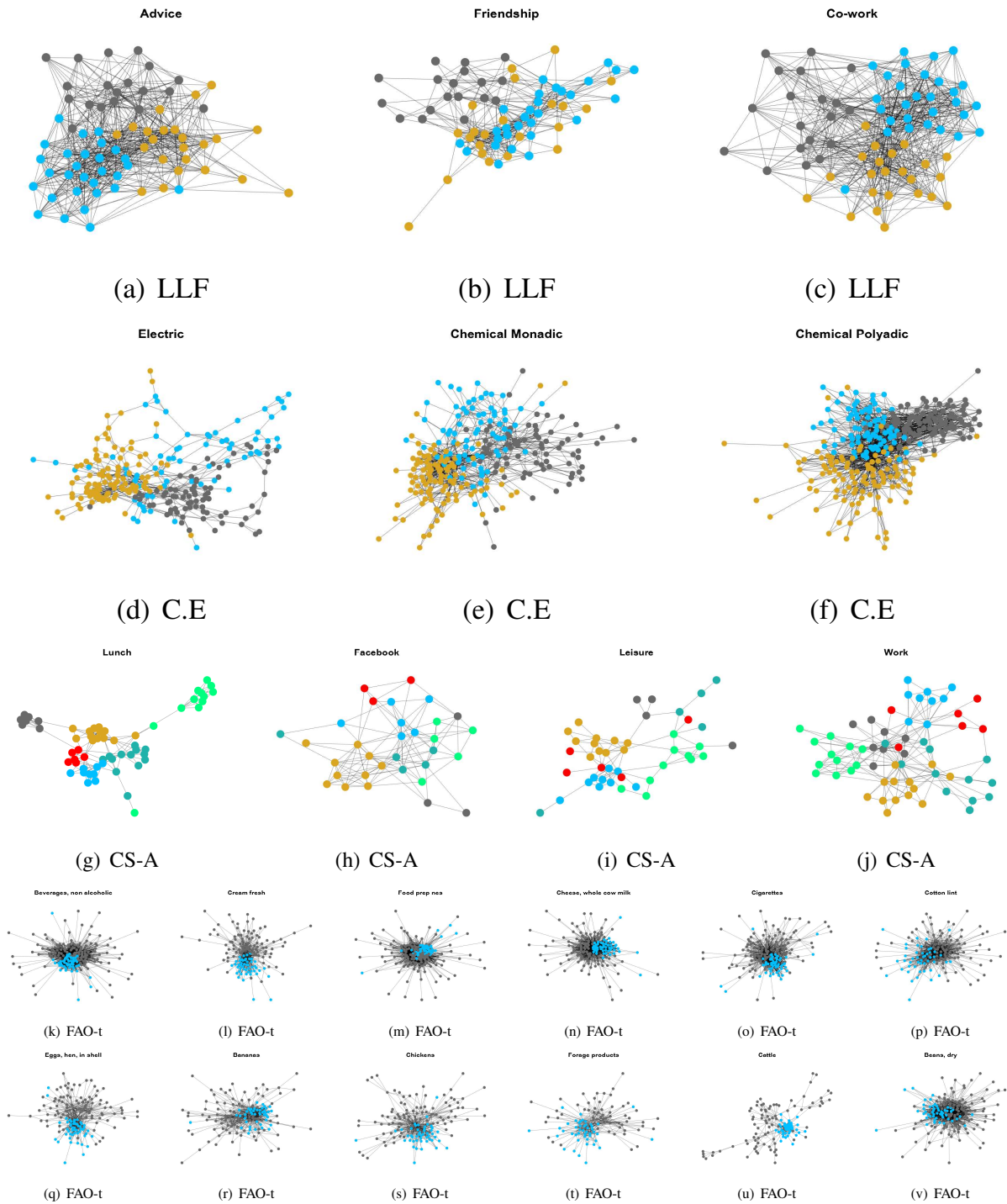


Figure 7: Visualization of the estimated community structure of the four real datasets. Only the largest connected graph for each network is displayed. The estimated communities for each multi-layer network are the same as those presented in Figure 6. We do not show the Coauthor layer of CS-A because it is too sparse. Colors indicate estimated communities.

Appendix A. Proofs

Proof of Lemma 1: For $i \in [n]$,

$$\begin{aligned}\mathcal{D}_\tau(i, i) &= \tau + \sum_{j \in [n]} \mathcal{S}(i, j) = \tau + \sum_{j \in [n]} \sum_{\ell \in [T]} \sum_{m \in [n]} \Omega_\ell(i, m) \Omega_\ell(j, m) = \tau + \sum_{j \in [n]} \sum_{\ell \in [T]} \sum_{m \in [n]} Z(i, :) B_\ell Z'(m, :) Z(j, :) B_\ell Z'(m, :) \\ &= \tau + Z(i, :) \sum_{j \in [n]} \sum_{\ell \in [T]} \sum_{m \in [n]} B_\ell Z'(m, :) Z(j, :) B_\ell Z'(m, :),\end{aligned}$$

and

$$\mathcal{S}(i, :) = \left(\sum_{\ell \in [T]} \Omega_\ell^2 \right)(i, :) = \left(\sum_{\ell \in [T]} Z B_\ell Z' Z B_\ell Z' \right)(i, :) = Z(i, :) \sum_{\ell \in [T]} B_\ell Z' Z B_\ell Z'.$$

Thus, if $\ell(i) = \ell(\bar{i})$, we have $\mathcal{D}_\tau(i, i) = \mathcal{D}_\tau(\bar{i}, \bar{i})$ and $\mathcal{S}(i, :) = \mathcal{S}(\bar{i}, :)$ for $i \in [n], \bar{i} \in [n]$, i.e., \mathcal{D}_τ has only K distinct diagonal elements and \mathcal{S} only has K distinct rows. By $\mathcal{L}_\tau = \mathcal{D}_\tau^{-\frac{1}{2}} \mathcal{S} \mathcal{D}_\tau^{-\frac{1}{2}} = U \Sigma U'$, we have $U = \mathcal{D}_\tau^{-\frac{1}{2}} \mathcal{S} \mathcal{D}_\tau^{-\frac{1}{2}} U \Sigma^{-1} \Rightarrow U(i, :) = \mathcal{D}_\tau^{-\frac{1}{2}}(i, i) \mathcal{S}(i, :) \mathcal{D}_\tau^{-\frac{1}{2}} U \Sigma^{-1} \Rightarrow U(i, :) = U(\bar{i}, :)$ if $\ell(i) = \ell(\bar{i})$.

For $k \in [K]$, choose any K nodes p_1, p_2, \dots, p_K such that $\ell(p_k) = k$. Let $\mathcal{I} = \{p_1, p_2, \dots, p_K\}$. Then, we have

$$Z(\mathcal{I}, :) = \begin{bmatrix} Z(p_1, :) \\ Z(p_2, :) \\ \vdots \\ Z(p_K, :) \end{bmatrix} = I. \text{ By basic algebra, we have } \mathcal{D}_\tau^{-\frac{1}{2}} Z = Z \mathcal{D}_\tau^{-\frac{1}{2}}(\mathcal{I}, \mathcal{I}).$$

Under the MLSBM, we get

$$U(\mathcal{I}, :) = \mathcal{D}_\tau^{-\frac{1}{2}}(\mathcal{I}, \mathcal{I}) \mathcal{S}(\mathcal{I}, :) \mathcal{D}_\tau^{-\frac{1}{2}} U \Sigma^{-1} = \mathcal{D}_\tau^{-\frac{1}{2}}(\mathcal{I}, \mathcal{I}) Z(\mathcal{I}, :) \left(\sum_{\ell \in [T]} B_\ell Z' Z B_\ell Z' \right) \mathcal{D}_\tau^{-\frac{1}{2}} U \Sigma^{-1} = \mathcal{D}_\tau^{-\frac{1}{2}}(\mathcal{I}, \mathcal{I}) \left(\sum_{\ell \in [T]} B_\ell Z' Z B_\ell Z' \right) \mathcal{D}_\tau^{-\frac{1}{2}} U \Sigma^{-1},$$

which gives that

$$Z U(\mathcal{I}, :) = Z \mathcal{D}_\tau^{-\frac{1}{2}}(\mathcal{I}, \mathcal{I}) \left(\sum_{\ell \in [T]} B_\ell Z' Z B_\ell Z' \right) \mathcal{D}_\tau^{-\frac{1}{2}} U \Sigma^{-1} = \mathcal{D}_\tau^{-\frac{1}{2}} Z \left(\sum_{\ell \in [T]} B_\ell Z' Z B_\ell Z' \right) \mathcal{D}_\tau^{-\frac{1}{2}} U \Sigma^{-1} = U.$$

Thus, $U = ZX$ with $X = U(\mathcal{I}, :)$. $XX' = (Z'Z)^{-1} = \text{diag}(1/n_1, 1/n_2, \dots, 1/n_K)$ because $U'U = I = X'Z'ZX$, i.e., X has orthogonal rows and $\|X(k, :)\|_F = 1/n_k$ for $k \in [K]$. This completes the proof.

Remark 4. Lemma 2.1 in (Lei & Rinaldo, 2015) can also prove this lemma. We explain this statement now. Set $H = \sum_{\ell \in [T]} B_\ell Z' Z B_\ell$. Since $Z'Z$ is a positive diagonal matrix, we have $\text{rank}(\mathcal{L}_\tau) = \text{rank}(H) = \text{rank}(\sum_{\ell \in [T]} B_\ell^2) = \text{rank}(\sum_{\ell \in [T]} \tilde{B}_\ell^2) = K$. Since $\mathcal{D}_\tau^{-\frac{1}{2}} Z = Z \mathcal{D}_\tau^{-\frac{1}{2}}(\mathcal{I}, \mathcal{I})$, we have $\mathcal{L}_\tau = \mathcal{D}_\tau^{-\frac{1}{2}} \mathcal{S} \mathcal{D}_\tau^{-\frac{1}{2}} = \mathcal{D}_\tau^{-\frac{1}{2}} \left(\sum_{\ell \in [T]} Z B_\ell Z' Z B_\ell Z' \right) \mathcal{D}_\tau^{-\frac{1}{2}} =$

$\mathcal{D}_\tau^{-\frac{1}{2}}\mathbf{Z}\mathbf{H}\mathbf{Z}'\mathcal{D}_\tau^{-\frac{1}{2}} = \mathbf{Z}\mathcal{D}_\tau^{-\frac{1}{2}}(\mathbf{I}, \mathbf{I})\mathbf{H}\mathcal{D}_\tau^{-\frac{1}{2}}(\mathbf{I}, \mathbf{I})\mathbf{Z}'$. Set $\tilde{\mathbf{H}} = \mathcal{D}_\tau^{-\frac{1}{2}}(\mathbf{I}, \mathbf{I})\mathbf{H}\mathcal{D}_\tau^{-\frac{1}{2}}(\mathbf{I}, \mathbf{I})$. We have $\mathcal{L}_\tau = \mathbf{Z}\tilde{\mathbf{H}}\mathbf{Z}'$, which shares the same form as the $\mathbf{P} = \Theta\mathbf{B}\Theta'$ in Lemma 2.1 (Lei & Rinaldo, 2015). Thus, results in Lemma 2.1 of (Lei & Rinaldo, 2015) also hold for the \mathbf{U} studied in this paper. ■

Proof of Theorem 1: Based on Assumption 2 and $\lambda_K(\mathbf{Z}'\mathbf{Z}) = n_{\min}$, we provide a lower bound of $|\lambda_K(\mathcal{L}_\tau)|$:

$$\begin{aligned} |\lambda_K(\mathcal{L}_\tau)| &= |\lambda_K(\mathcal{D}_\tau^{-\frac{1}{2}}\mathbf{S}\mathcal{D}_\tau^{-\frac{1}{2}})| \geq \lambda_K(\mathcal{D}_\tau^{-1})|\lambda_K(\mathbf{S})| = \frac{1}{\tau + \delta_{\max}}|\lambda_K(\mathbf{S})| = \frac{1}{\tau + \delta_{\max}}|\lambda_K(\sum_{l \in [T]} \Omega_l^2)| \\ &= \frac{1}{\tau + \delta_{\max}}|\lambda_K(\sum_{l \in [T]} \mathbf{Z}\mathbf{B}_l\mathbf{Z}'\mathbf{Z}\mathbf{B}_l\mathbf{Z}')| = \frac{\rho^2}{\tau + \delta_{\max}}|\lambda_K(\mathbf{Z}(\sum_{l \in [T]} \tilde{\mathbf{B}}_l\mathbf{Z}'\mathbf{Z}\tilde{\mathbf{B}}_l)\mathbf{Z}')| \geq \frac{\rho^2}{\tau + \delta_{\max}}\lambda_K(\mathbf{Z}'\mathbf{Z})|\lambda_K(\sum_{l \in [T]} \tilde{\mathbf{B}}_l\mathbf{Z}'\mathbf{Z}\tilde{\mathbf{B}}_l)| \\ &= O(\frac{\rho^2}{\tau + \delta_{\max}}\lambda_K^2(\mathbf{Z}'\mathbf{Z})|\lambda_K(\sum_{l \in [T]} \tilde{\mathbf{B}}_l^2)|) = O(\frac{\rho^2 n_{\min}^2 T}{\tau + \delta_{\max}}). \end{aligned}$$

Lemma 5.1 of (Lei & Rinaldo, 2015) says that there is an orthogonal matrix \mathbf{Q} such that

$$\|\mathbf{U} - \hat{\mathbf{U}}\mathbf{Q}\|_F \leq \frac{2\sqrt{2K}\|\mathbf{L}_\tau - \mathcal{L}_\tau\|}{|\lambda_K(\mathcal{L}_\tau)|}.$$

Using the lower bound of $|\lambda_K(\mathcal{L}_\tau)|$ gives

$$\|\mathbf{U} - \hat{\mathbf{U}}\mathbf{Q}\|_F = O(\frac{(\tau + \delta_{\max})\sqrt{K}\|\mathbf{L}_\tau - \mathcal{L}_\tau\|}{\rho^2 n_{\min}^2 T}).$$

By Lemma 2 in (Joseph & Yu, 2016) and Lemma 1, we know that for a small quantity $\delta > 0$, if

$$\frac{\sqrt{K}}{\delta}\|\mathbf{U} - \hat{\mathbf{U}}\mathbf{Q}\|_F(\frac{1}{\sqrt{n_k}} + \frac{1}{\sqrt{n_{\tilde{k}}}}) \leq \sqrt{\frac{1}{n_k} + \frac{1}{n_{\tilde{k}}}}, \text{ for } 1 \leq k < \tilde{k} \leq K, \quad (\text{A.1})$$

we have $\hat{f}_{RDS\alpha S} = O(\delta^2)$. If we set $\delta = \sqrt{\frac{2Kn_{\max}}{n_{\min}}}\|\mathbf{U} - \hat{\mathbf{U}}\mathbf{Q}\|_F$, we have

$$\begin{aligned} \frac{\sqrt{K}}{\delta}\|\mathbf{U} - \hat{\mathbf{U}}\mathbf{Q}\|_F(\frac{1}{\sqrt{n_k}} + \frac{1}{\sqrt{n_{\tilde{k}}}}) &= \sqrt{\frac{n_{\min}}{2n_{\max}}}(\frac{1}{\sqrt{n_k}} + \frac{1}{\sqrt{n_{\tilde{k}}}}) \leq \sqrt{\frac{n_{\min}}{2n_{\max}}}(\frac{1}{\sqrt{n_{\max}}} + \frac{1}{\sqrt{n_{\max}}}) = \sqrt{\frac{2n_{\min}}{n_{\max}^2}} \\ &= \sqrt{\frac{n_{\min}}{n_{\max}}\frac{1}{n_{\max}} + \frac{n_{\min}}{n_{\max}}\frac{1}{n_{\max}}} \leq \sqrt{\frac{1}{n_{\max}} + \frac{1}{n_{\max}}} \leq \sqrt{\frac{1}{n_k} + \frac{1}{n_{\tilde{k}}}}, \end{aligned}$$

which implies that $\hat{f}_{RDS\alpha G} = O(\delta^2) = O(\frac{Kn_{\max}\|\mathbf{U} - \hat{\mathbf{U}}\mathbf{Q}\|_F^2}{n_{\min}}) = O(\frac{K^2 n_{\max}(\tau + \delta_{\max})^2 \|\mathbf{L}_\tau - \mathcal{L}_\tau\|^2}{\rho^4 n_{\min}^5 T^2})$. Setting $\Theta = \sqrt{\rho}I$ in Lemma 3, we

get

$$\hat{f}_{RDS oG} = \frac{K^2 n_{\max}(\tau + \delta_{\max})^2}{\rho^4 n_{\min}^5 T^2} \left(O\left(\frac{\rho^2 n^2 T \log(n+T)}{(\tau + \delta_{\min})^2}\right) + O\left(\frac{\rho^4 n^2 T^2}{(\tau + \delta_{\min})^2}\right) + O\left(\frac{\rho^4 n^4 T^2 \log^2(n+T)}{(\tau + \delta_{\min})^4}\right) + O\left(\frac{\rho^8 n^4 T^4}{(\tau + \delta_{\min})^4}\right) \right).$$

■

Proof of Lemma 2: Under the MLDCSBM, $\mathcal{S} = \sum_{l \in [T]} \Omega_l^2 = \sum_{l \in [T]} \Theta Z \tilde{B}_l Z' \Theta^2 Z \tilde{B}_l Z' \Theta = \Theta Z (\sum_{l \in [T]} \tilde{B}_l Z' \Theta^2 Z \tilde{B}_l) Z' \Theta$ gives $\mathcal{L}_\tau = \mathcal{D}_\tau^{-\frac{1}{2}} \mathcal{S} \mathcal{D}_\tau^{-\frac{1}{2}} = \mathcal{D}_\tau^{-\frac{1}{2}} \Theta Z (\sum_{l \in [T]} \tilde{B}_l Z' \Theta^2 Z \tilde{B}_l) Z' \Theta \mathcal{D}_\tau^{-\frac{1}{2}}$. Set $\tilde{H} = \sum_{l \in [T]} \tilde{B}_l Z' \Theta^2 Z \tilde{B}_l$ and $\tilde{\Theta} = \mathcal{D}_\tau^{-\frac{1}{2}} \Theta$. $\tilde{\Theta}$ is a positive diagonal matrix. Thus, $\text{rank}(\mathcal{L}_\tau) = \text{rank}(\tilde{H}) = \text{rank}(\sum_{l \in [T]} \tilde{B}_l^2) = K$ since $Z' \Theta^2 Z$ is positive definite. Meanwhile, $\mathcal{L}_\tau = \tilde{\Theta} \tilde{H} Z' \tilde{\Theta} = U \Sigma U'$ gives $U = \tilde{\Theta} Z \tilde{H} Z' \tilde{\Theta} U \Sigma^{-1}$. Thus, $U_*(i, :) = \frac{U(i, :)}{\|U(i, :)\|_F} = \frac{\tilde{\Theta}(i, i) Z(i, :)}{\|\tilde{\Theta}(i, i) Z(i, :)\|_F} = \frac{Z(i, :)}{\|Z(i, :)\|_F}$, which implies that $U_*(\bar{i}, :) = U_*(i, :)$ if nodes \bar{i} and i are in the same community.

Define a diagonal matrix Δ as $\Delta(k, k) = \frac{\|\tilde{\Theta} Z(:, k)\|_F}{\|\tilde{\Theta}\|_F}$ and a matrix Γ as $\Gamma(:, k) = \frac{\tilde{\Theta} Z(:, k)}{\|\tilde{\Theta} Z(:, k)\|_F}$ for $k \in [K]$. Then $\Gamma' \Gamma = I$ and $\mathcal{L}_\tau = \|\tilde{\Theta}\|_F^2 \Gamma \Delta \tilde{H} \Delta \Gamma'$ hold. By Lemma 3 in (Qing & Wang, 2023b), this lemma holds.

Remark 5. Similar to Remark 4, we can also use Lemma 4.1 in (Lei & Rinaldo, 2015) to prove this lemma since $\mathcal{L}_\tau = \tilde{\Theta} Z \tilde{H} Z' \tilde{\Theta}$ shares the same form of the $P = \text{diag}(\psi) \Theta B \Theta' \text{diag}(\psi)$ in Lemma 4.1 of (Lei & Rinaldo, 2015).

■

Proof of Lemma 3: For $\|L_\tau - \mathcal{L}_\tau\|$, we have

$$\begin{aligned} \|L_\tau - \mathcal{L}_\tau\| &= \|\mathcal{D}_\tau^{-\frac{1}{2}} S \mathcal{D}_\tau^{-\frac{1}{2}} - \mathcal{D}_\tau^{-\frac{1}{2}} \mathcal{S} \mathcal{D}_\tau^{-\frac{1}{2}}\| = \|\mathcal{D}_\tau^{-\frac{1}{2}} S \mathcal{D}_\tau^{-\frac{1}{2}} - \mathcal{D}_\tau^{-\frac{1}{2}} S \mathcal{D}_\tau^{-\frac{1}{2}} + \mathcal{D}_\tau^{-\frac{1}{2}} S \mathcal{D}_\tau^{-\frac{1}{2}} - \mathcal{D}_\tau^{-\frac{1}{2}} \mathcal{S} \mathcal{D}_\tau^{-\frac{1}{2}}\| \\ &\leq \underbrace{\|\mathcal{D}_\tau^{-\frac{1}{2}} S \mathcal{D}_\tau^{-\frac{1}{2}} - \mathcal{D}_\tau^{-\frac{1}{2}} \mathcal{S} \mathcal{D}_\tau^{-\frac{1}{2}}\|}_{I1} + \underbrace{\|\mathcal{D}_\tau^{-\frac{1}{2}} (S - \mathcal{S}) \mathcal{D}_\tau^{-\frac{1}{2}}\|}_{I2}. \end{aligned}$$

As long as we can obtain the upper bounds of the two terms $I1$ and $I2$, we can bound $\|L_\tau - \mathcal{L}_\tau\|$. Now, we bound these two terms separately.

For the term $I1$, using the facts that $\|D^{-\frac{1}{2}} S D^{-\frac{1}{2}}\|$ and $\|D_\tau^{-1} D\| \leq 1$ gives

$$\begin{aligned} \|\mathcal{D}_\tau^{-\frac{1}{2}} S \mathcal{D}_\tau^{-\frac{1}{2}} - \mathcal{D}_\tau^{-\frac{1}{2}} \mathcal{S} \mathcal{D}_\tau^{-\frac{1}{2}}\| &= \|(I - \mathcal{D}_\tau^{\frac{1}{2}} \mathcal{D}_\tau^{-\frac{1}{2}}) \mathcal{D}_\tau^{-\frac{1}{2}} S \mathcal{D}_\tau^{-\frac{1}{2}} + \mathcal{D}_\tau^{-\frac{1}{2}} S \mathcal{D}_\tau^{-\frac{1}{2}} - \mathcal{D}_\tau^{-\frac{1}{2}} \mathcal{S} \mathcal{D}_\tau^{-\frac{1}{2}}\| \\ &\leq \|(I - \mathcal{D}_\tau^{\frac{1}{2}} \mathcal{D}_\tau^{-\frac{1}{2}}) \mathcal{D}_\tau^{-\frac{1}{2}} S \mathcal{D}_\tau^{-\frac{1}{2}}\| + \|\mathcal{D}_\tau^{-\frac{1}{2}} S (\mathcal{D}_\tau^{-\frac{1}{2}} - \mathcal{S} \mathcal{D}_\tau^{-\frac{1}{2}})\| \\ &= \|(I - \mathcal{D}_\tau^{\frac{1}{2}} \mathcal{D}_\tau^{-\frac{1}{2}}) \mathcal{D}_\tau^{-\frac{1}{2}} D^{\frac{1}{2}} D^{-\frac{1}{2}} S D^{-\frac{1}{2}} D^{\frac{1}{2}} \mathcal{D}_\tau^{-\frac{1}{2}}\| + \|\mathcal{D}_\tau^{-\frac{1}{2}} D^{\frac{1}{2}} D^{-\frac{1}{2}} S D^{-\frac{1}{2}} D^{\frac{1}{2}} (\mathcal{D}_\tau^{-\frac{1}{2}} - \mathcal{S} \mathcal{D}_\tau^{-\frac{1}{2}})\| \\ &= \|(I - \mathcal{D}_\tau^{\frac{1}{2}} \mathcal{D}_\tau^{-\frac{1}{2}}) \mathcal{D}_\tau^{-\frac{1}{2}} D^{\frac{1}{2}} \|\|D^{-\frac{1}{2}} S D^{-\frac{1}{2}}\| \|\|D^{\frac{1}{2}} \mathcal{D}_\tau^{-\frac{1}{2}}\| + \|\mathcal{D}_\tau^{-\frac{1}{2}} D^{\frac{1}{2}} \|\|D^{-\frac{1}{2}} S D^{-\frac{1}{2}}\| \|\|D^{\frac{1}{2}} (\mathcal{D}_\tau^{-\frac{1}{2}} - \mathcal{S} \mathcal{D}_\tau^{-\frac{1}{2}})\| \\ &= \|(I - \mathcal{D}_\tau^{\frac{1}{2}} \mathcal{D}_\tau^{-\frac{1}{2}}) \mathcal{D}_\tau^{-\frac{1}{2}} D^{\frac{1}{2}} \|\|D^{\frac{1}{2}} \mathcal{D}_\tau^{-\frac{1}{2}}\| + \|\mathcal{D}_\tau^{-\frac{1}{2}} D^{\frac{1}{2}} \|\|D^{\frac{1}{2}} (\mathcal{D}_\tau^{-\frac{1}{2}} - \mathcal{S} \mathcal{D}_\tau^{-\frac{1}{2}})\| \\ &= \|(I - \mathcal{D}_\tau^{\frac{1}{2}} \mathcal{D}_\tau^{-\frac{1}{2}}) \mathcal{D}_\tau^{-\frac{1}{2}} D^{\frac{1}{2}} \|\|D^{\frac{1}{2}} \mathcal{D}_\tau^{-\frac{1}{2}}\| + \|\mathcal{D}_\tau^{-\frac{1}{2}} D^{\frac{1}{2}} \|\|D^{\frac{1}{2}} (I - \mathcal{D}_\tau^{\frac{1}{2}} \mathcal{D}_\tau^{-\frac{1}{2}}) \mathcal{D}_\tau^{-\frac{1}{2}}\| \end{aligned}$$

$$\begin{aligned}
&\leq \|I - D_\tau^{\frac{1}{2}} \mathcal{D}_\tau^{-\frac{1}{2}}\| \|D_\tau^{-1} D\| + \|\mathcal{D}_\tau^{-\frac{1}{2}} D^{\frac{1}{2}}\| \|I - D_\tau^{\frac{1}{2}} \mathcal{D}_\tau^{-\frac{1}{2}}\| \|D_\tau^{-\frac{1}{2}} D^{\frac{1}{2}}\| \\
&= \|I - D_\tau^{\frac{1}{2}} \mathcal{D}_\tau^{-\frac{1}{2}}\| \|D_\tau^{-1} D\| + \|((I - D_\tau^{\frac{1}{2}} \mathcal{D}_\tau^{-\frac{1}{2}}) D_\tau^{-\frac{1}{2}} - D_\tau^{-\frac{1}{2}}) D^{\frac{1}{2}}\| \|I - D_\tau^{\frac{1}{2}} \mathcal{D}_\tau^{-\frac{1}{2}}\| \|D_\tau^{-\frac{1}{2}} D^{\frac{1}{2}}\| \\
&\leq \|I - D_\tau^{\frac{1}{2}} \mathcal{D}_\tau^{-\frac{1}{2}}\| \|D_\tau^{-1} D\| + (\|I - D_\tau^{\frac{1}{2}} \mathcal{D}_\tau^{-\frac{1}{2}}\| \|D_\tau^{-\frac{1}{2}} D^{\frac{1}{2}}\| + \|D_\tau^{-\frac{1}{2}} D^{\frac{1}{2}}\|) \|I - D_\tau^{\frac{1}{2}} \mathcal{D}_\tau^{-\frac{1}{2}}\| \|D_\tau^{-\frac{1}{2}} D^{\frac{1}{2}}\| \\
&= 2\|I - D_\tau^{\frac{1}{2}} \mathcal{D}_\tau^{-\frac{1}{2}}\| \|D_\tau^{-1} D\| + \|I - D_\tau^{\frac{1}{2}} \mathcal{D}_\tau^{-\frac{1}{2}}\|^2 \|D_\tau^{-1} D\| \\
&\leq 2\|I - D_\tau^{\frac{1}{2}} \mathcal{D}_\tau^{-\frac{1}{2}}\| + \|I - D_\tau^{\frac{1}{2}} \mathcal{D}_\tau^{-\frac{1}{2}}\|^2.
\end{aligned}$$

Since $\|I - D_\tau^{\frac{1}{2}} \mathcal{D}_\tau^{-\frac{1}{2}}\| \leq \max_{i \in [n]} |1 - \frac{\tau + \mathcal{D}(i, i)}{\tau + \mathcal{D}(i, i)}| \leq \frac{1}{\tau + \delta_{\min}} \max_{i \in [n]} |D(i, i) - \mathcal{D}(i, i)|$, according to Lemma 4, we obtain

$$\|D_\tau^{-\frac{1}{2}} S D_\tau^{-\frac{1}{2}} - \mathcal{D}_\tau^{-\frac{1}{2}} S \mathcal{D}_\tau^{-\frac{1}{2}}\| = O\left(\frac{\sqrt{\theta_{\max} \|\theta\|_1 \|\theta\|_F^2 T \log(n+T)}}{\tau + \delta_{\min}}\right) + O\left(\frac{\theta_{\max}^2 \|\theta\|_F^2 T}{\tau + \delta_{\min}}\right) + O\left(\frac{\theta_{\max} \|\theta\|_1 \|\theta\|_F^2 T \log(n+T)}{(\tau + \delta_{\min})^2}\right) + O\left(\frac{\theta_{\max}^4 \|\theta\|_F^4 T^2}{(\tau + \delta_{\min})^2}\right).$$

For the term $I2$, we have

$$\|\mathcal{D}_\tau^{-\frac{1}{2}} (S - \mathcal{S}) \mathcal{D}_\tau^{-\frac{1}{2}}\| \leq \|\mathcal{D}_\tau^{-1}\| \|S - \mathcal{S}\| = \frac{\|S - \mathcal{S}\|}{\tau + \delta_{\min}}.$$

When $\theta_{\max} \|\theta\|_1 \|\theta\|_F^2 T \geq \log(n+T)$, Lemma 4 of (Qing, 2024) gives

$$\|S - \mathcal{S}\| = O\left(\sqrt{\theta_{\max} \|\theta\|_1 \|\theta\|_F^2 T \log(n+T)}\right) + O\left(\theta_{\max}^2 \|\theta\|_F^2 T\right),$$

which gives

$$\|\mathcal{D}_\tau^{-\frac{1}{2}} (S - \mathcal{S}) \mathcal{D}_\tau^{-\frac{1}{2}}\| = O\left(\frac{\sqrt{\theta_{\max} \|\theta\|_1 \|\theta\|_F^2 T \log(n+T)}}{\tau + \delta_{\min}}\right) + O\left(\frac{\theta_{\max}^2 \|\theta\|_F^2 T}{\tau + \delta_{\min}}\right).$$

Finally, combining the bounds of the two terms $I1$ and $I2$ gives

$$\|L_\tau - \mathcal{L}_\tau\| = O\left(\frac{\sqrt{\theta_{\max} \|\theta\|_1 \|\theta\|_F^2 T \log(n+T)}}{\tau + \delta_{\min}}\right) + O\left(\frac{\theta_{\max}^2 \|\theta\|_F^2 T}{\tau + \delta_{\min}}\right) + O\left(\frac{\theta_{\max} \|\theta\|_1 \|\theta\|_F^2 T \log(n+T)}{(\tau + \delta_{\min})^2}\right) + O\left(\frac{\theta_{\max}^4 \|\theta\|_F^4 T^2}{(\tau + \delta_{\min})^2}\right).$$

■

Proof of Theorem 2: First, we have:

$$|\lambda_K(\mathcal{L}_\tau)| = |\lambda_K(\mathcal{D}_\tau^{-\frac{1}{2}} S \mathcal{D}_\tau^{-\frac{1}{2}})| \geq \frac{1}{\tau + \delta_{\max}} |\lambda_K(\sum_{i \in [T]} \Omega_i^2)| = \frac{1}{\tau + \delta_{\max}} |\lambda_K(\sum_{i \in [T]} \Theta Z \tilde{B}_i Z' \Theta^2 Z \tilde{B}_i Z' \Theta)|$$

$$= \frac{1}{\tau + \delta_{\max}} |\lambda_K(\Theta Z (\sum_{i \in [T]} \tilde{B}_i Z' \Theta^2 Z \tilde{B}_i) Z' \Theta)| \geq \frac{1}{\tau + \delta_{\max}} \theta_{\min}^2 n_{\min} |\lambda_K(\sum_{i \in [T]} \tilde{B}_i Z' \Theta^2 Z \tilde{B}_i)| = O\left(\frac{\theta_{\min}^4 n_{\min}^2 T}{\tau + \delta_{\max}}\right).$$

Combing the above lower bound of $|\lambda_K(\mathcal{L}_\tau)|$ with Lemma 5.1 of (Lei & Rinaldo, 2015), we get

$$\|U - \hat{U}\tilde{Q}\|_F = O\left(\frac{(\tau + \delta_{\max})\sqrt{K}\|L_\tau - \mathcal{L}_\tau\|}{\theta_{\min}^4 n_{\min}^2 T}\right),$$

where \tilde{Q} is orthogonal. Since $\|U_* - \hat{U}_*\tilde{Q}\|_F \leq \frac{2\|U - \hat{U}\tilde{Q}\|_F}{\gamma}$, where $\gamma = \min_{i \in [n]} \|U(i, :)\|_F$. By Lemma 2, we know that $\mathcal{L}_\tau = \tilde{\Theta} Z \tilde{H} Z' \tilde{\Theta}$ with $\tilde{\Theta} = \mathcal{D}_\tau^{-\frac{1}{2}} \Theta$. Set $\tilde{\theta}$ as an $n \times 1$ vector such that $\tilde{\theta}(i) = \tilde{\Theta}(i, i)$ for $i \in [n]$. Set $\tilde{\theta}_{\max} = \max_{i \in [n]} \tilde{\theta}(i)$ and $\tilde{\theta}_{\min} = \min_{i \in [n]} \tilde{\theta}(i)$. Since $\mathcal{L}_\tau = \tilde{\Theta} Z \tilde{H} Z' \tilde{\Theta}$ is the symmetric form of $\Omega = \Theta_r Z_r P Z_c' \Theta_c$ in Equation (3) of (Qing & Wang, 2023b), according to the analysis of Theorem 2 of (Qing & Wang, 2023b), $\frac{1}{\gamma} \leq \frac{\tilde{\theta}_{\max} \sqrt{n_{\max}}}{\tilde{\theta}_{\min}}$. For $\tilde{\theta}_{\max}$, we have $\tilde{\theta}_{\max} = \max_{i \in [n]} \tilde{\theta}(i) = \max_{i \in [n]} \tilde{\Theta}(i, i) = \max_{i \in [n]} (\mathcal{D}_\tau^{-\frac{1}{2}} \Theta)(i, i) \leq \frac{\theta_{\max}}{\sqrt{\tau + \delta_{\min}}}$. Similarly, $\tilde{\theta}_{\min} \geq \frac{\theta_{\min}}{\sqrt{\tau + \delta_{\max}}}$. Thus, we have $\frac{1}{\gamma} \leq \frac{\theta_{\max} \sqrt{(\tau + \delta_{\max}) n_{\max}}}{\theta_{\min} \sqrt{\tau + \delta_{\min}}}$, which gives that

$$\|U_* - \hat{U}_*\tilde{Q}\|_F = O\left(\frac{\theta_{\max}(\tau + \delta_{\max})^{1.5} \sqrt{K n_{\max}} \|L_\tau - \mathcal{L}_\tau\|}{\theta_{\min}^5 n_{\min}^2 T \sqrt{\tau + \delta_{\min}}}\right),$$

Combining Lemma 2 of (Joseph & Yu, 2016) with Lemma 2 gives that for $\tilde{\delta} > 0$, if

$$\frac{\sqrt{K}}{\tilde{\delta}} \|U_* - \hat{U}_*\tilde{Q}\|_F \left(\frac{1}{\sqrt{n_k}} + \frac{1}{\sqrt{n_{\tilde{k}}}}\right) \leq \sqrt{2}, \text{ for } 1 \leq \tilde{k} < k \leq K, \quad (\text{A.2})$$

$\hat{f}_{DC-RDSoS} = O(\tilde{\delta}^2)$. Setting $\tilde{\delta} = \sqrt{\frac{2K}{n_{\min}}} \|U_* - \hat{U}_*\tilde{Q}\|_F$ gives

$$\frac{\sqrt{K}}{\tilde{\delta}} \|U_* - \hat{U}_*\tilde{Q}\|_F \left(\frac{1}{\sqrt{n_k}} + \frac{1}{\sqrt{n_{\tilde{k}}}}\right) = \sqrt{\frac{n_{\min}}{2}} \left(\frac{1}{\sqrt{n_k}} + \frac{1}{\sqrt{n_{\tilde{k}}}}\right) \leq \sqrt{2}.$$

Thus, we have $\hat{f}_{DC-RDSoS} = O(\tilde{\delta}^2) = O\left(\frac{K \|U_* - \hat{U}_*\tilde{Q}\|_F^2}{n_{\min}}\right) = O\left(\frac{\theta_{\max}^2 (\tau + \delta_{\max})^3 K^2 n_{\max} \|L_\tau - \mathcal{L}_\tau\|^2}{\theta_{\min}^{10} (\tau + \delta_{\min}) n_{\min}^5 T^2}\right)$. By Lemma 3, we have

$$\begin{aligned} \hat{f}_{DC-RDSoS} &= \frac{\theta_{\max}^2 (\tau + \delta_{\max})^3 K^2 n_{\max}}{\theta_{\min}^{10} (\tau + \delta_{\min}) n_{\min}^5 T^2} \left(O\left(\frac{\theta_{\max} \|\theta\|_1 \|\theta\|_F^2 T \log(n+T)}{(\tau + \delta_{\min})^2}\right) + O\left(\frac{\theta_{\max}^4 \|\theta\|_F^4 T^2}{(\tau + \delta_{\min})^2}\right) + O\left(\frac{\theta_{\max}^2 \|\theta\|_1^2 \|\theta\|_F^4 T^2 \log^2(n+T)}{(\tau + \delta_{\min})^4}\right) \right) \\ &\quad + O\left(\frac{\theta_{\max}^8 \|\theta\|_F^8 T^4}{(\tau + \delta_{\min})^4}\right). \end{aligned}$$

■

Appendix B. One useful lemma

Lemma 4. *Under the same condition as Lemma 3, we have*

$$\max_{i \in [n]} |D(i, i) - \mathcal{D}(i, i)| = O(\sqrt{\theta_{\max} \|\theta\|_1 \|\theta\|_F^2 T \log(n+T)}) + O(\theta_{\max}^2 \|\theta\|_F^2 T),$$

with probability as least $1 - o(\frac{1}{n+T})$.

Proof of Lemma 4: By basic algebra, we have $\mathcal{D}(i, i) = \sum_{j \in [n]} \mathcal{S}(i, j) = \sum_{j \in [n]} \sum_{l \in [T]} \sum_{m \in [n]} \Omega_l(i, m) \Omega_l(j, m)$ and $D(i, i) = \sum_{j \neq i, j \in [n]} \sum_{l \in [T]} \sum_{m \in [n]} A_l(i, m) A_l(j, m)$, which give that

$$\begin{aligned} |D(i, i) - \mathcal{D}(i, i)| &= \left| \sum_{j \neq i, j \in [n]} \sum_{l \in [T]} \sum_{m \in [n]} (A_l(i, m) A_l(j, m) - \Omega_l(i, m) \Omega_l(j, m)) - \sum_{l \in [T]} \sum_{m \in [n]} \Omega_l^2(i, m) \right| \\ &\leq \left| \sum_{j \neq i, j \in [n]} \sum_{l \in [T]} \sum_{m \in [n]} (A_l(i, m) A_l(j, m) - \Omega_l(i, m) \Omega_l(j, m)) \right| + \theta_{\max}^2 \|\theta\|_F^2 T. \end{aligned}$$

For $j \neq i, j \in [n]$, we have

- $\mathbb{E}(A_l(i, m) A_l(j, m) - \Omega_l(i, m) \Omega_l(j, m)) = 0$ and $|A_l(i, m) A_l(j, m) - \Omega_l(i, m) \Omega_l(j, m)| \leq 1$.
- Set $\sigma^2 = \sum_{j \neq i, j \in [n]} \sum_{l \in [T]} \sum_{m \in [n]} \mathbb{E}((A_l(i, m) A_l(j, m) - \Omega_l(i, m) \Omega_l(j, m))^2)$. We have

$$\begin{aligned} \sigma^2 &= \sum_{j \neq i, j \in [n]} \sum_{l \in [T]} \sum_{m \in [n]} \Omega_l(i, m) \Omega_l(j, m) (1 - \Omega_l(i, m) \Omega_l(j, m)) \leq \sum_{j \neq i, j \in [n]} \sum_{l \in [T]} \sum_{m \in [n]} \theta(i) \theta(j) \theta^2(m) \leq \sum_{j \in [n]} \sum_{l \in [T]} \sum_{m \in [n]} \theta(i) \theta(j) \theta^2(m) \\ &\leq \theta_{\max} \sum_{l \in [T]} \sum_{j \in [n]} \sum_{m \in [n]} \theta(j) \theta^2(m) = \theta_{\max} \|\theta\|_1 \|\theta\|_F^2 T. \end{aligned}$$

By Theorem 1.4 (Tropp, 2012), for any $t \geq 0$,

$$\mathbb{P}\left(\left| \sum_{j \neq i, j \in [n]} \sum_{l \in [T]} \sum_{m \in [n]} (A_l(i, m) A_l(j, m) - \Omega_l(i, m) \Omega_l(j, m)) \right| \geq t \right) \leq \exp\left(\frac{-t^2/2}{\sigma^2 + t/3}\right) \leq \exp\left(\frac{-t^2/2}{\rho^2 n^2 T + t/3}\right).$$

Set $t = \frac{\sqrt{\alpha+1} + \sqrt{\alpha+19}}{3} \sqrt{\theta_{\max} \|\theta\|_1 \|\theta\|_F^2 T (\alpha+1) \log(n+T)}$ for any $\alpha \geq 0$. When $\theta_{\max} \|\theta\|_1 \|\theta\|_F^2 T \geq \log(n+T)$, we have

$$\mathbb{P}\left(\left| \sum_{j \neq i, j \in [n]} \sum_{l \in [T]} \sum_{m \in [n]} (A_l(i, m) A_l(j, m) - \Omega_l(i, m) \Omega_l(j, m)) \right| \geq t \right) \leq \exp\left(\frac{-t^2/2}{\rho^2 n^2 T + t/3}\right) \leq \frac{1}{(n+T)^{\alpha+1}}.$$

Setting $\alpha = 1$ completes the proof. ■

References

- Ali, H. T., & Couillet, R. (2018). Improved spectral community detection in large heterogeneous networks. *Journal of Machine Learning Research*, 18, 1–49.
- Ansari, A., Koenigsberg, O., & Stahl, F. (2011). Modeling multiple relationships in social networks. *Journal of Marketing Research*, 48, 713–728.
- Arroyo, J., Athreya, A., Cape, J., Chen, G., Priebe, C. E., & Vogelstein, J. T. (2021). Inference for multiple heterogeneous networks with a common invariant subspace. *Journal of Machine Learning Research*, 22, 1–49.
- Bakken, T. E., Miller, J. A., Ding, S.-L., Sunkin, S. M., Smith, K. A., Ng, L., Szafer, A., Dalley, R. A., Royall, J. J., Lemon, T. et al. (2016). A comprehensive transcriptional map of primate brain development. *Nature*, 535, 367–375.
- Boccaletti, S., Bianconi, G., Criado, R., Del Genio, C. I., Gómez-Gardenes, J., Romance, M., Sendina-Nadal, I., Wang, Z., & Zanin, M. (2014). The structure and dynamics of multilayer networks. *Physics Reports*, 544, 1–122.
- Chen, B. L., Hall, D. H., & Chklovskii, D. B. (2006). Wiring optimization can relate neuronal structure and function. *Proceedings of the National Academy of Sciences*, 103, 4723–4728.
- Cucuringu, M., Singh, A. V., Sulem, D., & Tyagi, H. (2021). Regularized spectral methods for clustering signed networks. *Journal of Machine Learning Research*, 22, 1–79.
- De Domenico, M., Nicosia, V., Arenas, A., & Latora, V. (2015). Structural reducibility of multilayer networks. *Nature Communications*, 6, 6864.
- Deng, S., Ling, S., & Strohmer, T. (2021). Strong consistency, graph laplacians, and the stochastic block model. *Journal of Machine Learning Research*, 22, 1–44.
- Fortunato, S. (2010). Community detection in graphs. *Physics Reports*, 486, 75–174.
- Fortunato, S., & Hric, D. (2016). Community detection in networks: A user guide. *Physics Reports*, 659, 1–44.
- Han, Q., Xu, K., & Airoldi, E. (2015). Consistent estimation of dynamic and multi-layer block models. In *International Conference on Machine Learning* (pp. 1511–1520). PMLR.
- Holland, P. W., Laskey, K. B., & Leinhardt, S. (1983). Stochastic blockmodels: First steps. *Social Networks*, 5, 109–137.
- Huang, X., Chen, D., Ren, T., & Wang, D. (2021). A survey of community detection methods in multilayer networks. *Data Mining and Knowledge Discovery*, 35, 1–45.
- Hubert, L., & Arabie, P. (1985). Comparing partitions. *Journal of Classification*, 2, 193–218.
- Jin, D., Yu, Z., Jiao, P., Pan, S., He, D., Wu, J., Philip, S. Y., & Zhang, W. (2021). A survey of community detection approaches: From statistical modeling to deep learning. *IEEE Transactions on Knowledge and Data Engineering*, 35, 1149–1170.
- Jin, J. (2015). Fast community detection by SCORE. *Annals of Statistics*, 43, 57–89.
- Joseph, A., & Yu, B. (2016). Impact of regularization on spectral clustering. *Annals of Statistics*, 44, 1765–1791.
- Karrer, B., & Newman, M. E. (2011). Stochastic blockmodels and community structure in networks. *Physical Review E*, 83, 016107.
- Kivelä, M., Arenas, A., Barthelemy, M., Gleeson, J. P., Moreno, Y., & Porter, M. A. (2014). Multilayer networks. *Journal of Complex Networks*, 2, 203–271.
- Lei, J., Chen, K., & Lynch, B. (2020). Consistent community detection in multi-layer network data. *Biometrika*, 107, 61–73.
- Lei, J., & Lin, K. Z. (2023). Bias-adjusted spectral clustering in multi-layer stochastic block models. *Journal of the American Statistical Association*, 118, 2433–2445.
- Lei, J., & Rinaldo, A. (2015). Consistency of spectral clustering in stochastic block models. *Annals of Statistics*, (pp. 215–237).
- Magnani, M., Micenkova, B., & Rossi, L. (2013). Combinatorial analysis of multiple networks. *arXiv preprint arXiv:1303.4986*, .
- Mucha, P. J., Richardson, T., Macon, K., Porter, M. A., & Onnela, J.-P. (2010). Community structure in time-dependent, multiscale, and multiplex networks. *Science*, 328, 876–878.

- Nepusz, T., Petróczy, A., Négyessy, L., & Bazsó, F. (2008). Fuzzy communities and the concept of bridgeness in complex networks. *Physical Review E*, *77*, 016107.
- Newman, M. E. (2002). Assortative mixing in networks. *Physical Review Letters*, *89*, 208701.
- Newman, M. E., & Girvan, M. (2004). Finding and evaluating community structure in networks. *Physical Review E*, *69*, 026113.
- Oselio, B., Kulesza, A., & Hero, A. O. (2014). Multi-layer graph analysis for dynamic social networks. *IEEE Journal of Selected Topics in Signal Processing*, *8*, 514–523.
- Paul, S., & Chen, Y. (2020). Spectral and matrix factorization methods for consistent community detection in multi-layer networks. *Annals of Statistics*, *48*, 230 – 250.
- Paul, S., & Chen, Y. (2021). Null models and community detection in multi-layer networks. *Sankhya A*, (pp. 1–55).
- Qin, T., & Rohe, K. (2013). Regularized spectral clustering under the degree-corrected stochastic blockmodel. *Advances in Neural Information Processing Systems*, *26*.
- Qing, H. (2024). Community detection by spectral methods in multi-layer networks. *arXiv preprint arXiv:2403.12540*, .
- Qing, H., & Wang, J. (2023a). Applications of dual regularized laplacian matrix for community detection. *Advances in Data Analysis and Classification*, (pp. 1–43).
- Qing, H., & Wang, J. (2023b). Community detection for weighted bipartite networks. *Knowledge-Based Systems*, *274*, 110643.
- Snijders, T. A., Pattison, P. E., Robins, G. L., & Handcock, M. S. (2006). New specifications for exponential random graph models. *Sociological Methodology*, *36*, 99–153.
- Strehl, A., & Ghosh, J. (2002). Cluster ensembles—a knowledge reuse framework for combining multiple partitions. *Journal of Machine Learning Research*, *3*, 583–617.
- Su, W., Guo, X., Chang, X., & Yang, Y. (2024). Spectral co-clustering in multi-layer directed networks. *Computational Statistics & Data Analysis*, (p. 107987).
- Tropp, J. A. (2012). User-friendly tail bounds for sums of random matrices. *Foundations of Computational Mathematics*, *12*, 389–434.
- Zhang, J., & Cao, J. (2017). Finding common modules in a time-varying network with application to the drosophila melanogaster gene regulation network. *Journal of the American Statistical Association*, *112*, 994–1008.